Rhine at risk?

te Linde, A.H.

2011

document version
Publisher's PDF, also known as Version of record

Rhine at risk?

Impact of climate change on low-probability floods in the Rhine basin and the effectiveness of flood management measures

Aline te Linde

Cover design and picture:
Sophie Valkenier

Stamps from the collection of:
Johan te Linde

Painting:
'Blick vom Isteiner Klotz rheinaufwärts richtung Basel', Peter Birmann, 1830

Printed by:
Wöhrmann Print Service, Zutphen

ISBN 978-90-8570-742-4

VRIJE UNIVERSITEIT

Rhine at risk?

Impact of climate change on low-probability floods in the Rhine basin and the effectiveness of flood management measures

ACADEMISCH PROEFSCHRIFT

ter verkrijging van de graad Doctor aan
de Vrije Universiteit Amsterdam,
op gezag van de rector magnificus
prof.dr. L.M. Bouter,
in het openbaar te verdedigen
ten overstaan van de promotiecommissie
van de faculteit der Aard- en Levenswetenschappen
op donderdag 12 mei 2011 om 13.45 uur
in de aula van de universiteit,
De Boelelaan 1105

door

Asselina Hermina te Linde

geboren te Deventer

promotor:	prof.dr J.C.J.H. Aerts
copromotoren:	prof.dr. A.J. Dolman
	dr. J.C.J. Kwadijk

leescommissie:	prof.dr A. Bronstert
	dr.ing. R. Lammersen
	prof.dr. H. Middelkoop
	prof.dr.ir. N.C. van de Giesen
	prof.dr. B.J.J.M. van den Hurk
	prof.dr.ir. P. Vellinga

This research was carried out at:

Institute for Environmental Studies (IVM)
Faculty of Earth and Life Sciences
VU University Amsterdam
De Boelelaan 1085 (visiting address)
De Boelelaan 1087 (postal address)
1081 HV Amsterdam
The Netherlands

and

Deltares
Rotterdamseweg 185 (visiting address)
P.O. Box 177 (postal address)
2600 MH Delft
The Netherlands

This research was carried out in the framework of the Dutch National Research Project 'Climate changes Spatial Planning' (wwww.klimaatvoorruimte.nl).

De zon smelt in de bergen de sneeuw om tot het water
dat glinsterend in beken de flanken langs krioelt
Zo kringelend haar weg zoekt tot het zich weer verzamelt
en stampend de rivier wordt die de rivier zich voelt

Kom dan blauwe regen
Val maar naar benee
Kom dan blauwe regen
Spoel me met je mee
Kom dan blauwe regen
Stroom me in de zee

Door dammen en met sluizen laat de rivier zich temmen
neemt boten zwaarbeladen en geschiedenissen mee
Ik zit hier aan de kade en luister naar de stemmen
die aan de einder opgaan in het water van de zee

Kom blauwe regen, De Dijk, 2005

Opgedragen aan wijlen Jaap Griede
(† 08–11–2006)

Preface

Fluvial flooding is a natural phenomenon creating the agricultural conditions and water availability relied on by humans. Fertile soils in river valleys are deposited by regular flooding, and river flows maintain the groundwater levels necessary for crop growth. Rivers provide water for drinking, industry, irrigation, sanitation, and transportation. Therefore, for centuries river valleys have attracted human settlement and economic development. However, flooding can be problematic in areas having such economic value.

Consequently, there are efforts to mitigate the hazard through the development of flood defense measures. Large rivers are often canalized to constrain their outwash, and valuable land may be protected by dikes. In highly-developed and densely populated river basins, such as the Rhine basin, flood defense measures have become sophisticated over the years. The question remains, however, whether current flood management practices are adequate in the face of climate change and further socio-economic development.

Flood frequency is low in river basins with existing flood management practices, leading to a certain level of safety. However, a flood event caused by dike failure or overtopping can still have major consequences. Flood mitigation approaches must optimize the balance between the investment costs of the flood defense system and the level of protection it affords. However, these costs and benefits vary both temporally and spatially. Public perception and socio-economic conditions influence this balance, but these factors and local policy change over time and may vary throughout a region, particularly in cross-boundary river basins. History has shown that a flooding event that causes damage and casualties often triggers or accelerates decision making of flood risk management. These decisions are then based on the best available knowledge at the time.

The future, however, is inherently uncertain and both the probability of a flood and the potential damage it may cause will change over time. This increases the challenge of designing flood defense measures. The potential for property damage and casualties depends on population increases, economic growth, and land-use changes in flood prone areas. The probability of flooding will vary according to changes in the river network and the hydraulic profile, the addition or removal of flood defense measures, and land-use changes such as deforestation and afforestation. Finally, climate change and variability have an influence on the flooding probability, primarily through altered temperature and precipitation, and thus needs to be considered in flood risk assessment and flood management. Erroneous or missing information may lead to undesirably low protection levels and possibly large hazards, while over-protection might lead to excess investment and possible unnecessary and undesirable landscape changes. Gathering essential information and knowledge to aid flood management requires extensive research and analysis.

The Rhine is a unique river basin for conducting research on the impact of climate change on extreme flood peaks and flood risk, and on the effectiveness of flood management measures. Seven countries share its basin and the Rhine has high economic value. Consequently, research and data on the river network and discharge, related land use, population wealth and other characteristics, soil properties, and meteorology are available for a considerable period of time. In addition, models exist for simulating the regions climate, hydrology and hydraulics, land use and flood damage potential.

It is expected that climate change will have a major impact on the discharge regime of the Rhine. Global warming may cause increased precipitation and earlier snow melt, with peak discharges likely to advance from spring to winter. This can increase the frequency of flooding and thus the flood risk. Therefore, for the riparian countries within the Rhine basin, establishing the effect of climate change on flood risk is an urgent issue.

Flood defense measures are designed to prevent the occurrence of extreme water levels at the so-called design discharge. However, there are methodological challenges in the design process due to the high safety standards in the Rhine basin (varying from 1/200 to 1/1250 per year). These high safety standards imply that defense measures need to protect against flood events that most likely have not yet been observed to date. Thus, the estimation of the probability and duration of design flood events is subject to scientific debate, in particular when considering climate change scenarios.

In Europe, water management is moving away from a flood defense approach to a more risk management based approach, which takes both the probability and the potential consequences of flooding into account. To aid in the planning of a flood risk management approach, basin-wide information is needed on the current probability of flooding, maximum water levels of extreme flood peaks, and the potential dam-

age from flooding. In addition, methods are needed to estimate the effect of climate and socio-economic changes on future trends in flood risk. However, modeling the impact of climate change in order to estimate the probability of flooding and test the effectiveness of flood management measures entails various difficulties and uncertainties. Improvements to this modeling process have received a great deal of attention in current research. Nonetheless, to date, no attempt has been made to estimate future flood risks on a basin-wide scale for the Rhine basin. In short: is the Rhine at risk?

In this thesis, I will describe methods for optimizing the simulation of the discharge regime and flood-peak probability in the Rhine basin, for present conditions and under future climate change. This thesis will also provide estimates for future flood risk related to different climate change and socio-economic scenarios. In addition, I will show how these methods can be applied to test the effectiveness of flood management measures in the Rhine basin. Finally, I will reflect on the implications of the results and provide new insight into the uncertainties in flood risk estimation in the Rhine basin. These are different to how these uncertainties are currently perceived. The conclusions are relevant for flood management decision making. Before specifying the objective and research questions of this thesis, the background, key questions, and available research methods are introduced and specified for the Rhine basin.

Contents

List of Figures

List of Tables

Chapter 1

Introduction

1.1 Problem definition

1.1.1 Economic loss due to floods

According to the United Nations, within two decades nearly 60% of humanity will live in urban areas (UN-HABITAT, 2008). More than two-thirds of the world's large cities are vulnerable to rising sea levels and river discharges, exposing $\sim$ 400 million people to the risk of extreme floods and storms (Nicholls et al., 2008). In the past decades, the number of fatalities and the economic loss caused by floods have increased considerably worldwide (Munich Re AG, 2008). This increase can be attributed to either climate change (Vellinga et al., 2001), population growth, or the increase in wealth in low-lying and often densely populated deltas (Bouwer et al., 2007; Pielke Jr. et al., 2008), or a combination of these causes.

In Europe, floods cause about 38% of the total economic losses due to natural hazards, making it, together with windstorms, the most costly type of natural disaster (EEA, 2008). In recent decades, Europe suffered over 100 major damaging fluvial floods, including catastrophic floods along the Danube and Elbe rivers in 2002 and 2006 (Thieken et al., 2005), the summer floods in 2007 in Great-Britain, and more recently in 2010 along the Wisla and Oder in Poland and Germany. Between 1970

and 2006, floods have caused some 1300 fatalities, the displacement of more than half a million people and at least €110 billion of economic losses (normalized to 2006 values) (Barredo, 2009).

The Rhine has a long flood history that caused casualties and severe damage (Glaser and Stangl, 2003; Blackbourn, 2006). Floods in 1993 and 1995 resulted in €1.4 and €2.7 billion damage, respectively (Engel, 1997; Brakenridge and Anderson, 2008). The probabilities of occurrence for the 1993 and 1995 events are relatively high and have been estimated at 1/25 and 1/50 per year, respectively (Te Linde et al., 2010). The peak discharges in those events resulted from heavy, long lasting rainfall in the uplands of the Middle and Lower Rhine, combined with mild temperatures that caused premature melting of snow (Caspary, 1996).

The largest riverine flood in the Netherlands in the 20st century occurred in 1926 (12 600 m^3/s at Lobith, Figure 1.1). In January 1995, the peak discharge reached 11 885 m^3/s at Lobith (Figure 1.2), and parts of Germany flooded. Within the Netherlands, 250 000 people were evacuated, but against expectations, the Dutch dikes held (Bezuyen and van Duin, 1998; Disse and Engel, 2001). To illustrate how hazardous floods can be in the Rhine basin, Herget and Meurs (2010) used historical descriptions of flood events and marks of maximum water levels on buildings to estimate that an exceptional event in the year 1374 reached almost 24 000 m^3/s at Cologne (Figure 1.2). Sprong (2009), however, estimated a peak discharge maximum of $\sim$ 18 000 m^3/s for the same event. Regardless, this level is still 50% higher than the discharge during the peak event of 1995. The question remains: what is the probability that such a flood event reoccurs, and what will then be the consequences?

1.1.2 Flood frequency and climate change

The Fourth Assessment report by the Intergovernmental Panel on Climate Change indicates that global warming will intensify the global hydrological cycle (IPCC, 2007b). As a consequence, the magnitude and frequency of extreme precipitation events is expected to increase, which may lead to increased probability of floods (Milly et al., 2005; Christensen and Christensen, 2007; Kundzewicz et al., 2007).

In North-West Europe, both from observations and prediction models a climate change-induced trend can be derived towards wetter winter conditions and increasing flood frequencies (EEA, 2008). In several rivers, the frequency of what are now considered 100-year floods may double in the future (Dankers and Feyen, 2008).

In the Lower Rhine, the peak discharge is likely to advance from spring to winter, as warming temperatures increase precipitation volumes and cause earlier snow melts (Middelkoop et al., 2001; Pfister et al., 2004). These impacts from climate change are projected to increase the mean winter discharge by 5–30% and decrease the mean

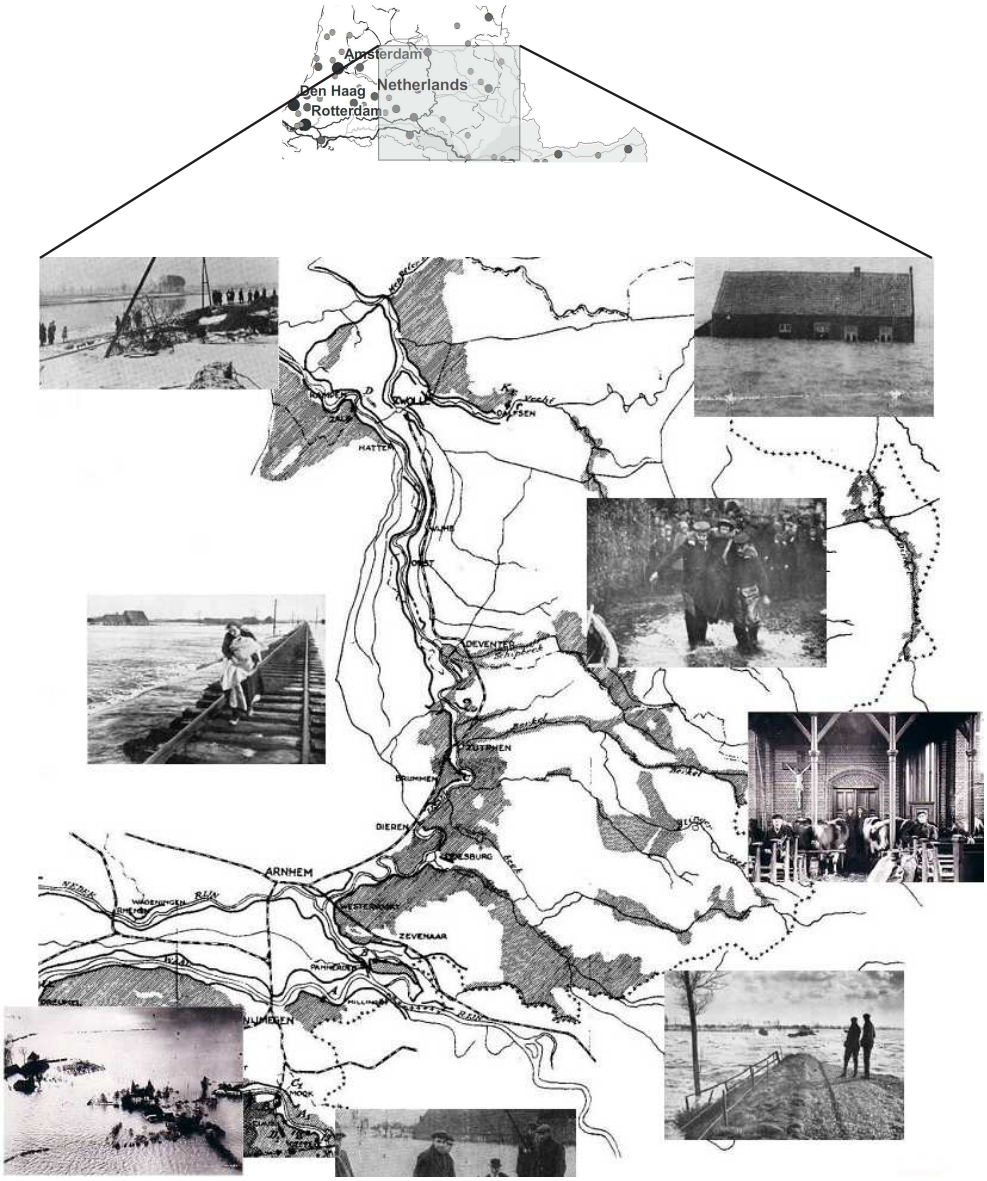

Figure 1.1: Map displaying the flood extent of the 1926 flooding in the Netherlands. The pictures are for the same event.

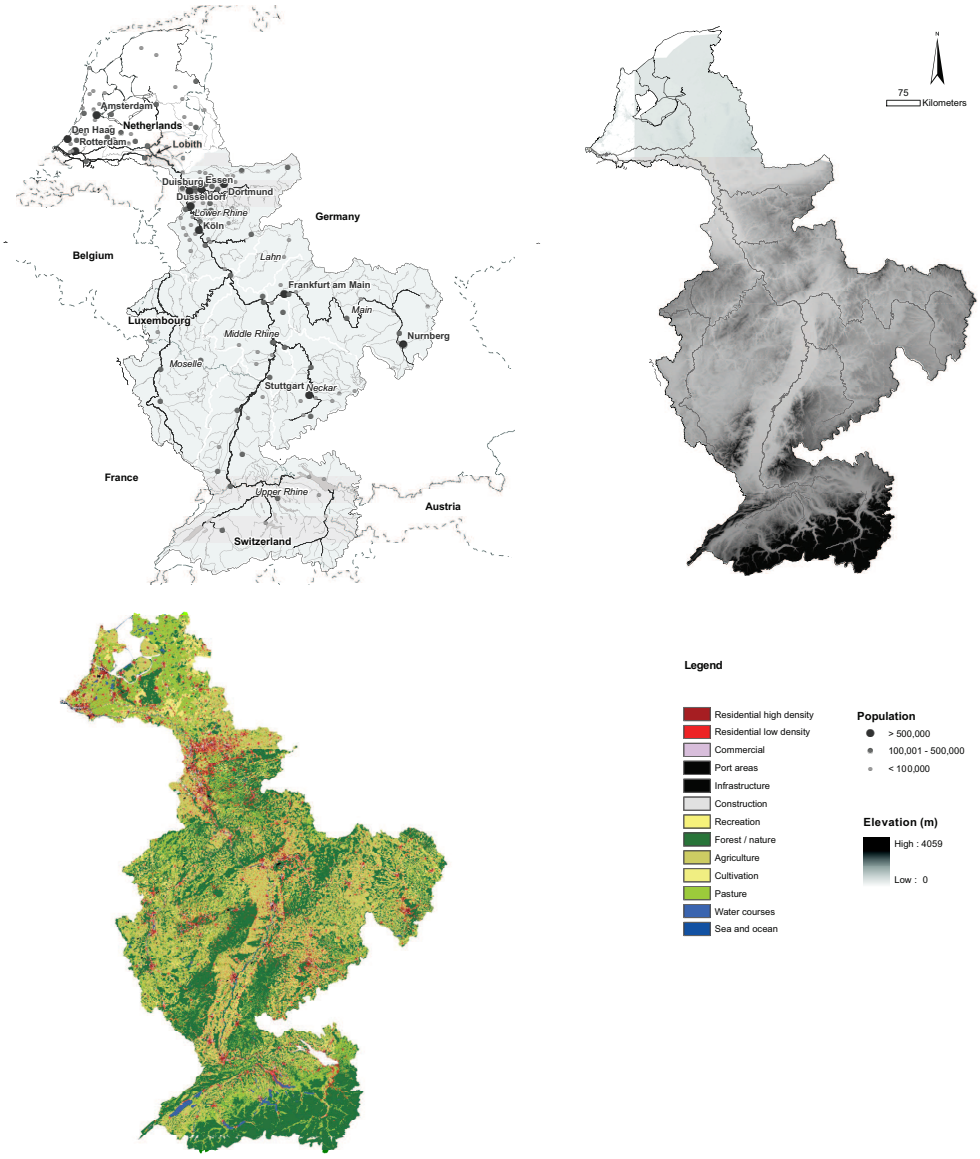

Figure 1.2: Maps of the Rhine basin: a) sub-basins and major cities, b) elevation, and c) land use.

summer discharge by 0–45% (e.g. Kwadijk, 1993; Buishand and Lenderink, 2004). As a consequence, the 1/1250 per year flood event (which is the design discharge for the Dutch embankments) at the gauging station of Lobith is estimated to increase from 16 000 m^3/s at present to somewhere between 16 500 and 19 500 m^3/s by 2050 (Kwadijk and Middelkoop, 1994; Grabs, 1997; Shabalova et al., 2003; Vellinga et al., 2008). This will increase the flood risk (Hooijer et al., 2004; Pinter et al., 2006). However, existing studies on flood risk in the Rhine basin have several shortcomings related to addressing low probability flood events. This research, therefore, aims to provide new methods and approaches to better understand the mechanisms and impacts of low probability floods in the Rhine basin.

1.1.3 Towards flood risk management

In several countries such as the Netherlands and Germany, there is a trend in flood management to convert from flood prevention (limited to controlling the water) to flood risk management which in addition considers the consequences of a potential flooding event (Plate, 2002; Merz et al., 2004; Büchele et al., 2006; ISFD4, 2008; Merz et al., 2010). Flood risk is defined in this thesis as the product of probability and potential damage, i.e., the expected loss per year (Smith, 2001). This trend arose from awareness that continued socio-economic development behind flood defenses increases the flood risk. De Moel et al. (2011) explain that not only the amount of economic and social capital has increased, but that developments behind flood defenses are occurring increasingly in more dangerous places, because the safer locations are already occupied.

In Europe, the tendency towards flood risk management is stimulated by the EU Flood Directive (EU, 2007a), which was enacted on 26 November 2007. It sets out several actions for member states such as initiating flood risk assessments, the development of flood risk maps, and the preparation of basin-wide risk management plans, which have to be completed by the end of 2015. Many member states in Europe have already collated information and maps for flood hazard (areas at risk of damage), but information and maps for flood risk are still rare (De Moel et al., 2009). The EU Green Paper on adaptation to climate change (EU, 2007b) also stresses the importance of looking beyond defensive measures.

The Dutch government has focused for many years on flood protection (Ten Brinke et al., 2008), with a recent cautious policy shift that considers the probabilities and consequences of flooding due to failure of flood defenses (Ministry of Transport, Public Works and Water Management, 2006a). In Germany, Samuels et al. (2006) found that at the federal level, flood risk management is also shifting away from flood protection to a more holistic approach that includes spatial planning and damage reduction. In practice, though, this new approach is difficult to implement, as most *Bundesländer*

draw up their own water management plans and use conventional methods of flood defense (Becker et al., 2007).

Historical research revealed that river canalization and the implementation of flood defense measures in upstream parts of the Rhine basin directly affected and often increased flood risk downstream (Blackbourn, 2006). Neighboring countries in the Rhine basin see the advantage of cross-boundary cooperation, but so far they have been reluctant to transfer their political influence to the International Commission for the Protection of the Rhine (ICPR) (Aerts and Droogers, 2004; Hooijer et al., 2004). Additional research on flood risk, climate change, and the identification of effective adaptation measures in the Rhine basin can optimize future and cross-boundary river basin management.

1.2 The Rhine

1.2.1 Basin characteristics

With a length of 1320 km and a river basin area of 185 000 km^2, the Rhine is one of the larger rivers of North-West Europe (Belz et al., 2007). The river basin covers parts of Switzerland, Austria, Liechtenstein, France, Luxembourg, Germany, and the Netherlands. The main tributaries of the Rhine are the Neckar, Main, Mosel, Lahn, and Sieg (Figure 1.2). The river basin can be subdivided in five sections using geographical and geological features (Preusser, 2008). The first section is the Alpine mountains where the river originates. Second is the Upper Rhine from Basel (where the flood plain is used for agriculture) up to Mainz. Several cities exist along the Rhine branch in this section. Third is the Middle Rhine between Mainz en Bonn, which is hilly. In this section the Rhine flows through a narrow gorge. Fourth is the Lower Rhine, which is densely urbanized. From here, the flood prone area widens until it becomes a river delta in the Netherlands (fifth section) (Hooijer et al., 2004). About 50% of the basin is used for agriculture, and 15% for urban or suburban uses. The remainder is forest and otherwise fallow lands (Wessel, 1995; Eberle et al., 2005) (Figure 1.2).

The Rhine is extensively used for inland shipping (Jonkeren et al., 2007; CCNR, 2009) and connects one of the world's largest sea ports, Rotterdam, to the inland European markets (Figure 1.3). The river also provides water for cooling energy plants, and for industrial, domestic, and agricultural purposes (Grabs, 1997). The Rhine basin is one of the most heavily industrialized areas in the world. It has 58 million inhabitants, of which 10.7 million live in flood prone areas that are protected by dikes (ICPR, 2001).

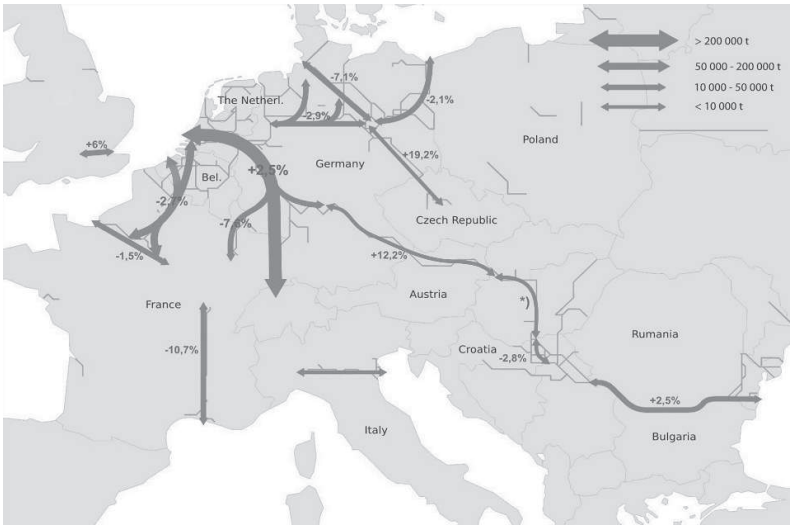

Figure 1.3: Inland waterway transport flows in Europe in 2007. Percentages show the increase in shipped tons in 2007 from 2006 (Source: CCNR (2009)).

1.2.2 Discharge characteristics and flood peak generation

The average discharge of the Rhine at the German Dutch border is 2200 m^3/s and the maximum discharge since observations began in 1901 was 12 600 m^3/s, at Lobith in 1926. Both rainfall and melt water contribute to discharge generation, depending on the season (Pinter et al., 2006; Uehrlinger et al., 2009). Extreme floods in the Lower Rhine mainly occur during the winter period. Research on historical floods in the Rhine basin shows that the most extreme peaks resulted from large meteorologic low-pressure systems that slowly crossed the basin while releasing great amounts of rainfall over several days (Beersma et al., 2008). Frozen soil can contribute to more extreme peaks, as it prevents rainfall from infiltrating the ground (Engel, 1997). In addition, the sudden melting of snow and frozen soil has been reported to increase flooding (Disse and Engel, 2001).

1.2.3 Flood defense measures

In order to protect vital economic activities in the Rhine basin, flood risk management has been primarily limited to flood defense measures. Dikes, first constructed in the 17^{th} century, have been widened and heightened (Lammersen et al., 2002). To force incision and reduce the flooding of the Upper Rhine, the river was straightened between 1817 and 1890 (Blackbourn, 2006), which shortened the river between Basel and Worms from 354 to 273 km (Silva et al., 2001).

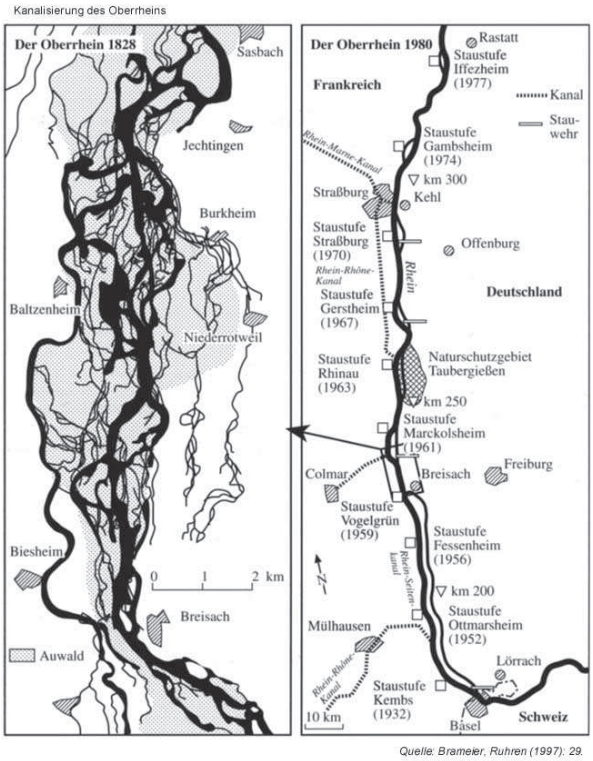

Figure 1.4: Canalization of the Upper Rhine.

The drastic rectification to tame the Upper Rhine was designed by an engineer named Tulla in the early 19$^{\text{th}}$ century. Although his plans had been ready for several decades, to his frustration they were not agreed upon by authorities, even though technology was sufficiently advanced for their implementation. His great project was realized finally with the changing institutional and political background in the riparian states of the Upper Rhine after the French Revolution (Blackbourn, 2006).

From 1928 to 1977, the Upper Rhine was further canalized to aid shipping and the construction of hydro-electric power stations (Figure 1.4). As a result, floods moved faster through this section of the Rhine, and peak water levels rose higher. To counteract this undesired effect, Germany and France agreed in 1982 to implement retention measures in and along the Upper Rhine. From 1851 to 1990 dramatic changes were also made in the Lower Rhine. Dikes were built, meanders were cut-off, and the river was secured with groynes (Silva et al., 2001).

Since then, flood management in the Netherlands and Germany has gone through several phases of institutional cooperation, which have been mainly triggered by extreme

events (Becker et al., 2007). The safety levels of the embankments vary between the different riparian countries of the Rhine basin. In the eastern part of the Netherlands, embankments are designed to withstand floods that occur on average once in 1250 years (now estimated at 16 000 m^3/s at Lobith (Ministry of Transport, Public Works and Water Management, 2006b); whereas in Germany, safety levels are set at 1/200 to 1/500 per year (Lammersen, 2004). Thus, floods may occur upstream in Germany, while being prevented by the Dutch dike system downstream (Gudden, 2004; Apel et al., 2006).

The flood peaks in 1993 and 1995 were an important wake-up call in the Netherlands. During these flood peaks, dike stability was considered weak and reached a point where safety could no longer be guaranteerd which led to the evacuation of 250 000 people, even though the observed discharges were much lower than the design discharge for those areas (12 000 m^3/s vs. 16 000 m^3/s). Since then, dikes have been strengthened and heightened up to their design levels (Ministry of Transport, Public Works and Water Management, 1995).

After the floods in 1993 and 1995, discussions on flood frequency and protection increased basin wide. A Ministers conference in February 1995, attended by representatives of all countries sharing the Rhine basin, resulted in the Action Plan on Floods, which is under the mandate of the International Commission for the Protection of the Rhine (ICPR, 1998). This plan has four goals: (1) to reduce flood risk by 10% in 2005 and by 25% in 2020, as compared with 1995; (2) to reduce extreme flood stages by 30 cm in 2005 and by 70 cm in 2020, as compared with 1995; (3) to raise awareness of flood risks; and (4) to improve flood forecasting. Measures to reduce flood stages were targeted mainly at upstream retention methods in the tributaries and the creation of extra retention volume by inundation polders along the main Rhine branch. In the Netherlands, instead of new dike reinforcements and dike raise, the government decided to create 'Room for the River', by widening and deepening flood planes (Ministry of Transport, Public Works and Water Management, 2006c). Figure 1.5 shows an overview of the flood reduction measures that can be implemented along the Rhine in the Netherlands.

In 2005, an evaluation of the Action Plan on Floods revealed that, with current climate conditions, neither the lowered flood risk nor the reduced flood stages targets were met (ICPR, 2005a). It was also uncertain whether the original plan adequately addressed the latest climate change projections. Hooijer et al. (2004) suggested that a lower flood risk in the Rhine basin could be achieved easier through damage reduction and spatial planning than by flood defense measures. However, this assumption is not yet confirmed by research, and there is a need to test the effectiveness of additional flood management measures by considering the impact of climate change on extreme flood peaks.

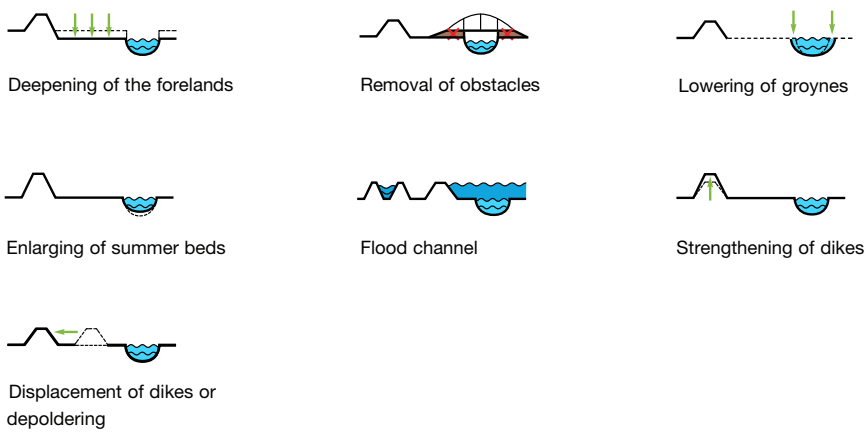

Figure 1.5: Measures in the Dutch Spatial Planning Key Decision 'Room for the River'.

1.3 Available research and remaining challenges

1.3.1 Simulating the effect of climate change on extreme flood peaks

To estimate the impact of climate change on future flood-peak probabilities, researchers must understand relevant and often complex relationships, processes, and thresholds in climate and hydrological systems, while accounting for the shortcomings and uncertainties in their modeling tools. The prediction of the impacts of climate change on the probabilities of extreme flood peaks requires many steps, including downscaling the output of general circulation models, simulating runoff, and conducting an extreme value analysis. All steps are concisely explained below.

GCMs and RCMs

In its Special Report on Emission Scenarios (SRES), the IPCC used different assumptions for economic development to define a set of greenhouse gas (GHG) emission scenarios (IPCC, 2000). They range from a world with regional economies and local solutions for environmental sustainability (low scenario, B1), to a global market economy with high growth rates and fossil fuel intensive energy technologies (high scenario, A2). Based on these emission scenarios, General Circulation Models (GCMs) were used to model weather characteristics at a global scale up to the year 2100 (Covey et al., 2003). This resulted in different scenarios for global warming (Figure 1.6).

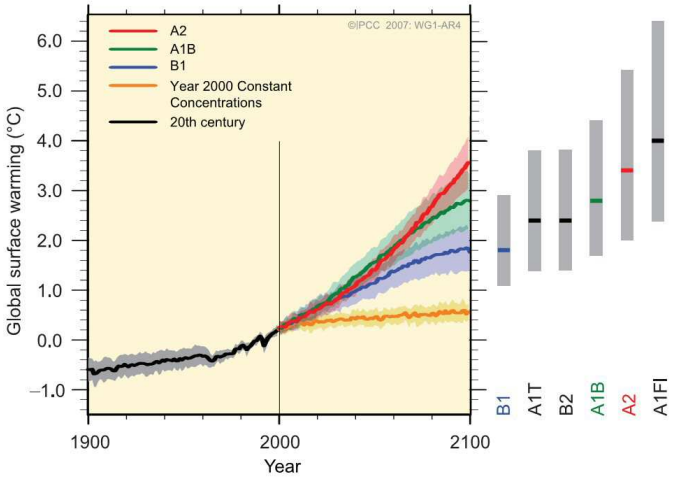

Figure 1.6: IPCC SRES scenarios for global warming (IPCC, 2000).

However, for subcontinental basins like the Rhine, the spatial resolution of a GCM is inadequate for forcing a hydrological model, and downscaling is required. The grid size of a GCM varies between 1 ° and 2 °, which at the latitude of the Rhine is about 100–200 km north-south and 80–160 km east-west. Consequently, the Rhine basin is only covered by a few GCM grid cells. Downscaling can be done by perturbing the historical series with the average change in climate parameters; this is referred to as the 'delta change' approach (Lenderink et al., 2007a; Te Linde, 2007). Downscaling can also be done statistically based on a reference period (Jacob et al., 2008), or dynamically using regional climate models (RCMs) that are nested within a GCM (e.g. Wilby et al., 2000; Jacob, 2001; Kay et al., 2006). The latter is known as the direct forcing approach.

Different climate models typically result in different climate projections and often simulate different changes in weather characteristics; this provides a first indication of the uncertainties involved (Horton et al., 2006; Menzel et al., 2006; Prudhomme, 2006; Lenderink et al., 2007b). The performance of climate models can be tested against observational data, and it is found that most RCMs underestimate the high rainfall extremes (Pitman and Perkins, 2007). A bias-correction on RCM output data using historical time series data is necessary to obtain meaningful input for hydrological models (Leander et al., 2008; Bakker and Van den Hurk, 2009). Methods for downscaling and bias-correction are continuously improving and different methods now exist to transform RCM output to hydrological input. There is not yet a consensus on which method is preferred: the robust but simple delta change approach, or the less robust (bias-corrected) direct RCM output, which provides more detailed

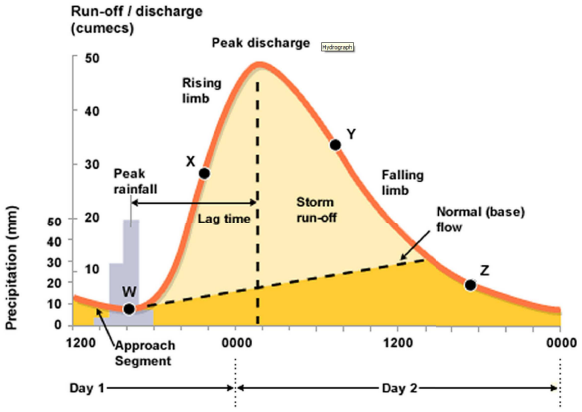

Figure 1.7: Hydrological response to precipitation (Bitesize, 2010).

information on the temporal and spatial changes (Wilby et al., 2000; Lenderink et al., 2007b).

Runoff simulation

The meteorological data series obtained from models describe both a reference situation and future scenarios of precipitation and temperature characteristics. The next step is to simulate the hydrological response to these climate change scenarios. However, this is not as straightforward as it seems. RCMs and hydrological models overlap each other in simulating land surface processes such as evaporation and discharge generation. Hydrologists and meteorologists are investigating methods to match the observed complexity in hydrological and meteorological processes with the necessary simplification in modeling tools at different scales (e.g. Koster et al., 2000).

Similar to climate models, there are many hydrological models to choose from. The hydrological response to a precipitation event can be visualized by a hydrograph (Figure 1.7). The hydrological community has devoted a great deal of attention in the last few decades to the understanding of hydrological processes and their representation in rainfall-runoff models (e.g. Refsgaard, 1996; Seibert, 1999; Perrin et al., 2000; Liu and Todini, 2002; Booij, 2003; Wagener et al., 2003; Troy et al., 2007). For an overview of benchmark papers since 1933 describing discharge generation processes, see Beven (2006b).

However, in the Rhine basin, our understanding of the discharge generating processes is still inadequate, and modeling results for the current hydrological situation at basin scale are only of moderate quality (Weerts, 2003; Bogaard et al., 2005). For example, there is an ongoing debate on the utility of more complex distributed models that at-

tempt to describe all physical processes at high resolutions, including soil-atmosphere feedback processes, as opposed to relatively simple lumped model approaches (e.g. Beven, 2001; Savenije, 2001; Bergström et al., 2002; Beven, 2006a; Sivakumar, 2008). In theory, physically-based or land surface models that describe soil-atmosphere feedback processes are preferred in climate impact analyses (Hurkmans et al., 2008). The question remains whether in practice they are easily applied and perform better than lumped model approaches.

The flood routing scheme of most hydrological models is generally insufficient for providing detailed information on flood wave propagation and peak water levels in low gradient river stretches, where floodplain inundation plays an important role (Chow, 1959). Engineers have developed hydrodynamic models that are capable of simulating the necessary detailed information on flood peak behavior in river channels much better (e.g. Delft Hydraulics, 2005). These models are used for planning of hydraulic structures, they are well calibrated using observations and scale models, and their performance is less subject to scientific debate than is the mathematical description of hydrological processes. However, these models require detailed information on hydraulic profiles and roughness parameters and involve intensive computing. Thus, hydrodynamic models are not applied within the vast majority of climate impact studies on discharge behavior, creating a gap in our understanding when planning flood management measures that aim to consider future climate change.

Also, the hydrological models currently applied in climate impact studies generally disregard the consequences of upstream flooding in Germany and France. Lammersen (2004) showed that extreme flood peaks can be topped off and delayed significantly in the downstream parts of the Rhine basin due to flooding in upstream areas having lower safety levels than the Dutch dike system. However, it is sometimes argued that as a response to flooding, safety levels and dikes in upstream areas might be raised in the future (Silva, 2003). Consequently, this effect has not been further investigated and is ignored at present in flood management strategies in the Lower Rhine in Germany and the Netherlands.

Extreme flood peaks

To test the effectiveness of flood management measures, the understanding of peak flow generation processes is essential. The consideration of climate change requires estimates of changes in the probability and magnitude of extreme flood peaks, which is far from trivial. For very rare extreme events (i.e., a probability of 1/200 per year or less), this often requires hydrological or statistical modeling of substantially higher discharges than are observed. As a result, these models are used far outside their calibrated range, introducing considerable uncertainties (Refsgaard, 1997; Klemeš, 2000a,b; Katz, 2002; Sivakumar, 2005; Garrett and Müller, 2008).

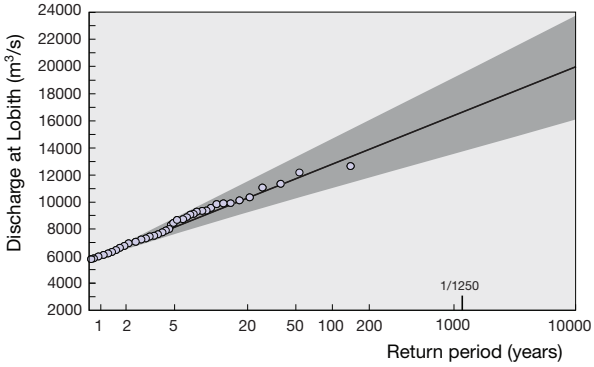

Figure 1.8: Statistical extrapolation to obtain the design discharge at Lobith at a return period of 1250 years and the 90% confidence intervals of the extreme value distribution fit (Silva et al., 2001).

Two approaches exist to estimate discharge volumes at design standards (i.e. 1/200 per year or less) that exceed historical observation records (i.e. 100 years). The most commonly used approach is to extrapolate an extreme value distribution fit of observed peak events to the desired safety standards (Shaw, 2002, Figure 1.8). This assumes stationarity of the observed data record, which implies fluctuations within an unchanging natural system as described by a static probability density function. However, in 100 years, both meteorological conditions and the river basin change, violating the principle of stationarity and increasing the uncertainty associated with the statistical extrapolation (Milly et al., 2008).

In an alternative approach, a weather generator can be used to create long, resampled time series of climate change scenarios as input for the hydrological models. These long time series then contain extreme events with very low probabilities (1/200 per year or less). Although research on the performance of such an approach to estimate design discharges is available (e.g. De Wit and Buishand, 2007; Leander, 2009), the design discharge at 1/1250 per year in the Netherlands is estimated by statistical extrapolation (Figure 1.8), which results in 90% confidence intervals at $16\,000\,\mathrm{m}^3/\mathrm{s}$ of $\pm\ 3000\,\mathrm{m}^3/\mathrm{s}$. These confidence intervals, however, are ignored in decision making (Ministry of Transport, Public Works and Water Management, 2006b).

Human intervention and the nonlinear and complex system of climate change further undermine the basic assumption of stationarity in water systems (Pielke Sr. et al., 2009). In response, Sivapalan and Samuel (2009) proposed a shift from traditional flood frequency analysis, based on stationarity, towards a new process-based approach (McMillan and Brasington, 2008) for flood estimation and the assessment of flooding probabilities. In this approach, the impact of climate change and the changes in river geometry and land use due to human influence are parameterized in models, in an

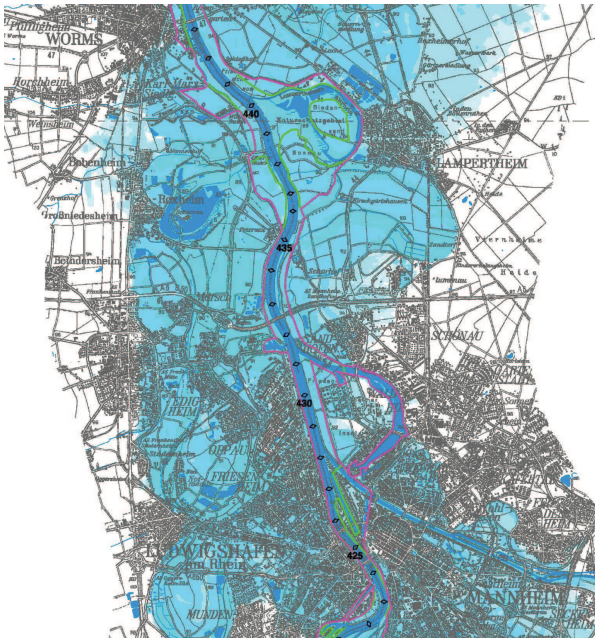

Figure 1.9: Inundation depth map between Ludwigshafen and Worms.

attempt to physically describe extreme situations and the consequences of changed conditions. Only recently have efforts been made to apply a process-based approach to climate impact studies (Raff et al., 2009).

1.3.2 Estimating potential damage and future flood risk

In flood risk management, the combined influence of socio-economic development and climate change presents a major challenge to water managers. Not only is it necessary to limit flood probabilities, but managers must also assess measures to alleviate the consequences of a flood. Examples of these measures are spatial planning (to avoid urban development in risky places), flood damage insurance, and early warning systems (Schanze et al., 2006). Spatial adaptation and flood defense measures may need to last for several decades; thus, their planning and management requires insight in likely future necessities. Also, flood risk is dynamic, due to changes in both land use and flood probability; this requires consideration of future impacts on flood risk. Worldwide, only a few studies have examined the potential future increase in disaster losses, accounting for both climate and socio-economic change (Bouwer, 2010).

To date, the most comprehensive overview on flood damage in the Rhine basin is the Rhine Atlas of the ICPR (Figure 1.9), which maps the overall direct damage potential (ICPR, 2001). However, it is not designed to derive information on current flood risk (probability times damage), nor future basin-wide flood risk estimations under socio-economic, land use, and climate changes.

The consequences due to flooding can be extensive and varied, and may be categorized into direct and indirect damage (Merz et al., 2010). Another distinction is made between tangible and intangible loss, depending on whether or not they can be monetized. Tangible direct loss includes damage to private and public property and infrastructure. Human suffering due to loss of life or injuries is an example of an intangible direct loss. Damage due to evacuation and disruption of economic activities is referred to as an indirect loss (Jonkman, 2007). Another example of an indirect loss is the loss of value suffered by any remaining real estate due to the flooding event (Daniel et al., 2009).

Direct economic damage is an important indicator for the severity of a flooding event, and is often monetized by insurance companies or others. In this thesis I focus on direct economic damage as a part of flood risk. The potential damage in flood prone areas is calculated by combining land-use and damage models, which may vary widely in scale and accuracy (e.g. Thieken et al., 2005; Klijn et al., 2007).

1.4 Objective and research questions

The central aim of this thesis is to assess the effect of climate and socio-economic change on flood risk in the Rhine basin and to improve existing simulation methods. The focus is on the estimation of the probability of flooding and the development of cross-boundary flood management measures to cope with expected changes. This objective will be achieved by addressing the following questions:

1. Does a physically-based land-surface model perform better than a conceptual rainfall-runoff model when simulating the effect of climate change on the discharge regime?
2. How can we optimally use climate change scenarios of precipitation and temperature to estimate expected changes in low-probability flood peak events?
3. What is the present basin-wide flood risk, how will it change up to 2030, and what is the relative contribution of climate and socio-economic change to this risk?
4. Which flood management measures are most effective in reducing flood stages and flood frequency on a basin-wide scale?

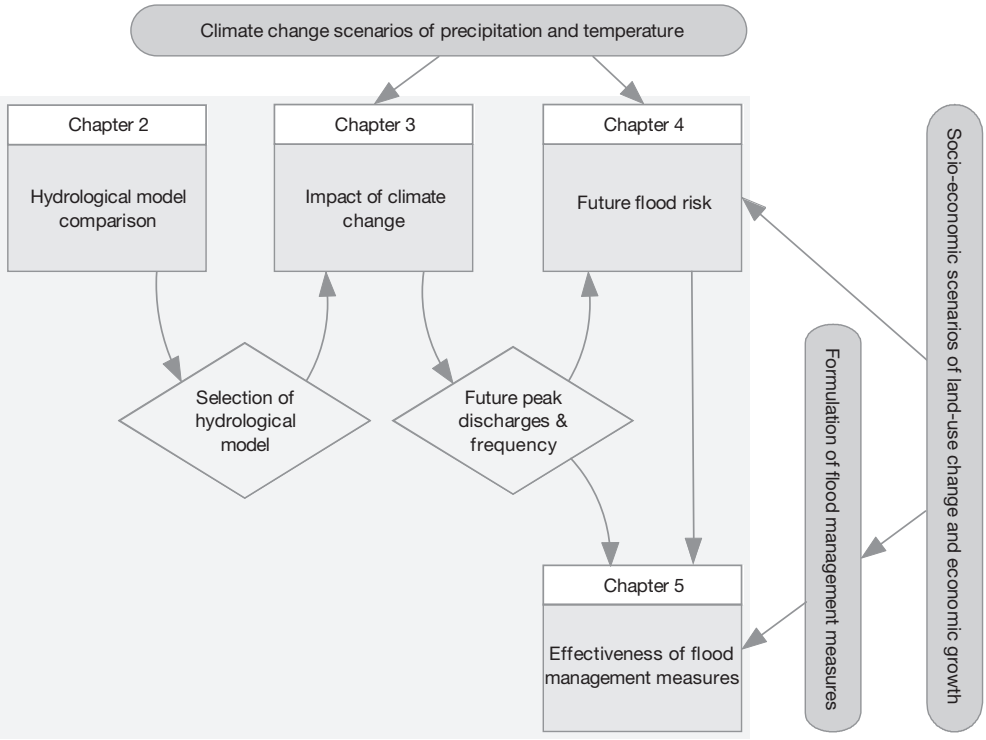

Figure 1.10: Outline of the thesis.

1.5 Thesis outline

A schematic of the chapters of this thesis is provided in Figure 1.10. Chapter 1 provides the problem definition and available research, concisely describes the Rhine basin, and sets out the main objectives and research questions.

Chapter 2 compares the performance of two hydrological models of different complexity and process description. The models are evaluated on their ability to simulate (peak) discharge on a sub-basin and basin-wide scale, using observed discharge series and different meteorological datasets. The result determines which rainfall-runoff model is best used in the remainder of the research.

In Chapter 3, future changes to the discharge regime are simulated and future flood-peak probabilities are estimated, using resampled climate modeling data. The resampling was performed to obtain a long time series of 1000 (when possible 10 000) years of daily discharge, representing hydrological conditions in the reference climate and in the climate predicted for 2050. This allows us to describe a certain state of the system using a process-based approach, in which changes in rainfall-runoff processes are

simulated due to altered meteorological conditions from climate change. These long time series reduce statistical uncertainty when estimating low probability flood-peak events. Different methods to transform the regional climate model (RCM) output to a hydrological model input were used and compared.

Chapter 4 provides estimates of future flood risk (the product of probability and potential damage) in the Rhine basin. Socio-economic scenarios, a land-use model and a damage model are used together to estimate current and future damage in flood prone areas. Only direct economic losses are considered, since most available data pertains to direct damage. Combined with earlier results on how flood peak probabilities change with climate, flood risk is assessed and spatially differentiated along the main Rhine branch.

In Chapter 5, the effectiveness of flood management measures on peak discharges is evaluated assuming a climate change scenario for the year 2050. Here, we extend the process-based simulation of discharge with a hydrodynamic component. Also, the effect of upstream flooding in Germany on flood stages downstream in the Netherlands is estimated using an ensemble of synthetic flood waves and a combination of a hydrological and hydrodynamic model.

Chapter 6 summarizes the results of previous chapters and addresses the four research questions. The main conclusions are presented and recommendations are made for further research.

Chapter 2

Comparing model performance of two rainfall-runoff models using different atmospheric forcing data sets

Te Linde, A.H., Aerts, J.C.J.H., Hurkmans, R.T.W. and Eberle, M., 2008. Comparing model performance of two rainfall-runoff models in the Rhine basin using different atmospheric forcing data sets. *Hydrololgy and Earth System Sciences*, 12: 943–957.

Abstract

Due to the growing wish and necessity to simulate the possible effects of climate change on the discharge regime on large rivers such as the Rhine in Europe, there is a need for well performing hydrological models that can be applied in climate change scenario studies. There exists large variety in available models and there is an ongoing debate in research on rainfall-runoff modeling on whether or not physically based distributed models better represent observed discharges than conceptual lumped model approaches do. In addition, it is argued that Land Surface Models (LSMs) carry the potential to accurately estimate hydrological partitioning, because they solve the coupled water and energy balance. In this Chapter, the hydrological models HBV and VIC were compared for the Rhine basin by testing their performance in simulating discharge. Overall, the semi-distributed conceptual HBV model performed much better than the distributed land surface model VIC (E=0.62, r^2=0.65 vs. E=0.31, r^2=0.54 at Lobith). It is argued here that even for a well-documented river basin such as the Rhine, more complex modeling does not automatically lead to better results.

Moreover, it is concluded that meteorological forcing data has a considerable influence on model performance, irrespectively to the type of model structure and the need for ground-based meteorological measurements is emphasized.

2.1 Introduction

It is expected that climate change will have major implications for the discharge regime of many rivers around the world (Kundzewicz et al., 2007). Changes in seasonal discharge are projected for river basins in mid-latitude regions, such as the Rhine basin in Europe. Seasonal discharge will most likely shift to more discharge in winter and less discharge in summer, and the frequencies of floods and droughts are expected to increase (Kwadijk, 1993; Middelkoop et al., 2001; Buishand and Lenderink, 2004). Recent climate change research focuses on simulating changes in the magnitude and frequencies of flood events using different models that are either developed for scenario studies, real time flood forecasting, or both (Van Deursen, 2006; Te Linde, 2007). Our understanding of the discharge generating processes in the Rhine basin, though, is still deficient and modeling results for describing the current hydrological situation at basin scale are of moderate quality. For instance, extreme events inside the calibrated range are both over and underestimated and it is difficult to separate the effects of errors in input data and model structure (Weerts, 2003). This increases the inherent uncertainty when using models outside their calibrated range, as is common practice in climate scenarios studies. Thus there is a need for a well performing hydrological model on extreme events that can be applied in various climate scenario studies, but there exists large variety in available models. Since these issues are common in applications of hydrological modeling in other regions as well, we chose to compare two rainfall-runoff models for the Rhine basin with divergent model structures.

The semi-distributed conceptual model HBV (Hydrologiska Byråns Vattenbalansavdelning) (Bergström, 1976; Lindström et al., 1997) has been applied in multiple studies for the Rhine basin since 1999 by both the German Federal Institute of Hydrology and the Dutch Ministry of Transport, Public Works and Water Management (Mülders et al., 1999; Weerts and Van der Klis, 2004; Eberle et al., 2005). However, the HBV model does not exactly describe all the physical processes that are believed to be of major importance for the simulation of timing and magnitude of extreme flood and drought events (Schär et al., 1998; Ward and Robinson, 1990). Potential evaporation, for example, is calculated using the Penman-Wendling approach based on temperature and sunshine duration (Eberle et al., 2005) while more innovative methods are available using coupled water and energy balance simulations. Recently the state of the art distributed land surface model (LSM) VIC (Variable Infiltration Capacity) (Liang et al., 1994) has been applied on the Rhine basin (Hurkmans et al., 2008), which does describe all relevant land surface processes, including the energy balance,

and therefore carries the potential to estimate hydrological partitioning more accurately than the HBV model does. Because of a realistic representation of evaporation processes in land surface models such as done within VIC, Troy et al. (2007) argue that these types of models are inevitable when performing climate and land use change scenario studies.

However, the application of a distributed land surface model such as VIC at a macroscale river basin, such as the Rhine basin, is still a highly simplified representation because of its spatial resolution. Even when using a very fine grid, in the order of tens or hundreds of meters and by that sabotaging calculation time, it will never represent actual processes that vary at a scale of trees and ditches (Uhlenbrook, 2003) and the actual heterogeneity of hydrological processes. Considering the required input data and computer capacity, the question remains whether more complex and demanding models such as VIC can be preferred over simpler, conceptual water balance models such as HBV. A better understanding of the use and capacity of different hydrological models would enhance the confidence in future climate scenario studies using these hydrological models. An uncertainty analysis of all processing steps from climate scenarios via downscaling methods to hydrological modeling is required. Estimating uncertainty of model simulations starts with analyzing model performance using historical data. In this view, the goal of this Chapter is to compare the hydrological models HBV and VIC by testing their performance for simulating historical discharge. Based on the performance of both models, a recommendation can be made for the type of hydrological model to be preferred for climate change scenario studies.

Since both models have a different physical structure resulting from a different theoretical background, the divergent concepts in rainfall-runoff modeling are first addressed in Section 2.2. In Section 2.3, the models and study area are described. In Section 2.4, the methods that are used for comparing atmospheric forcing data and model performance are explained, whereupon the results are presented in Section 2.5. Finally, the results are discussed and several conclusions are drawn in Section 2.6.

2.2 Divergent concepts in rainfall-runoff modeling

There is an ongoing debate in research on rainfall-runoff modeling on the utility of more complex distributed models that aim to describe all physical processes, including soil-atmosphere feedback processes. In the last decades the hydrologic community has devoted a great deal of attention to the understanding of hydrological processes and their representation by means of physically based, distributed models. The general idea of physically based, distributed modeling is that it represents reality better than lumped model approaches, as it takes into account spatial information and even more important, it uses physical law (mass balance and energy equations) to describe the

hydrological processes (Refsgaard, 1996; Reggiani and Schellekens, 2003). However, it is well recognized that the available approaches are often still far from providing a satisfactory representation of rainfall-runoff transformation (Bergström et al., 2002). A lot of work remains in identifying different runoff response mechanisms and to characterize the key state variables during calibration (Perrin et al., 2000; Uhlenbrook et al., 1999; Wagener et al., 2003). This should be done by extensive and long duration field observations, using the growing availability of radar and space high-resolution datasets, improving physical descriptions and refining grid size. Examples of physically based, distributed models are SHE (Abbott et al., 1986), FLOWSIM (Rientjes and Zaadnoordijk, 2000), WASIM-ETH (Schulla and Kaspar, 2006), LARSIM (Ludwig and Bremicker, 2006), REW (Reggiani et al., 1998, 1999), LISFLOOD (De Roo et al., 1998, 2000), TOPKAPI (Liu and Todini, 2002) and tRIBS (Vivoni, 2003). Related to these models are land surface model (LSMs). The original purpose of LSMs was to represent the land surface in (regional) climate simulations used for climate models and numerical weather prediction (Liang et al., 1994). Recently, LSMs have been used for streamflow forecasting as well. By solving both the water and energy balance, LSMs are able to exploit a larger part of the information provided by regional climate model output (Hurkmans et al., 2008), which is an advantage in climate change scenario studies where regional climate model (RCM) output is used. But because of the complex model structure and the large number of parameters in LSMs, they are generally difficult to parameterize. Furthermore, in most of these distributed modeling approaches, it remains difficult to represent processes occurring at scales smaller than the grid or element scale. The VIC model therefore offers sub-grid scale variation in vegetation and soil characteristics (Liang et al., 1994).

On the other hand, some researchers advocate a more straightforward hydrologic approach claiming that more complex modeling does not always lead to better results. Depending on dominant processes, data availability, scale and application of the model, one should select the appropriate modeling approach which can result in using a very simple model (Booij, 2003; Seibert, 1999). When formulating their famous and widely used performance criterion, Nash and Sutcliffe (1970) already warned for the risk of over-parameterized models. In recent years, the debate on model complexity versus model performance has intensified again and Beven (2001, 2002a,b) goes a step further and critically analyzed the constraints of distributed modeling. The perfect hydrological model that represents reality accurately will never exist, as there will always remain necessary approximations of processes and parameters at the model element scale. Beven (2001) claims that the ongoing pursue to a realistic representation has led to unjustified determinism in many distributed modeling applications and a lack of recognition of the problems of distributed modeling such as nonlinearity, scale and equifinality (which arises when many different parameter sets give equally good results). Furthermore, Savenije (2001) states that the large number of parameters in distributed models make it possible to represent hydrological behav-

ior well for the current situation, but due to over-parameterization these models are not the right tools to describe what will happen if certain characteristics of the basin change, such as land use or soil characteristics. Savenije (2001) suggests to further develop a new data-based top down approach (Jothityangkoon et al., 2001) in which relatively simple basin response functions describe complex hydrological processes at scales with sufficient level of aggregation. It consists of beginning with a large time step and gradually introducing the complexity required to meet the needs of shorter time steps. This resembles the conceptual approach of already long-existing water balance models like Sacramento, HBV and RhineFlow (Van Deursen and Kwadijk, 1993). Bogaard et al. (2005) argue that the main challenges in understanding discharge generating processes appear to be related to the scale of the processes. Micro scale hydrological processes are highly heterogeneous, non-linear and interconnected, with the consequence that upscaling from micro- to basin scale and subsequent parameterization is practically impossible. In conclusion, hydrologists are looking for answers to match the observed complexity at the plot-scale, with the apparent simplicity that arises at the basin scale. Comparing the HBV and VIC models, having opposed model structures, for their performance in a well-documented river basin like the Rhine basin, will add to the debate on divergent concepts in hydrological modeling.

2.3 Model description and study area

2.3.1 VIC

The Variable Infiltration Capacity (VIC) model (Liang and Zhenghui, 2001; Liang et al., 1994) is a distributed, macro-scale land surface model with a physically based soil-vegetation-atmosphere transfer scheme (SVATS), which solves both the water and energy balance. It is distinguished from other SVATS by its focus on runoff processes. These are represented through the variable infiltration curve, a parameterization of the effects of sub-grid variability in soil moisture holding capacity, from which the model takes its name, and a representation of non-linear baseflow. Routing of surface runoff and baseflow is done by the algorithm developed by Lohmann et al. (1996). A more extensive description of the modeling scheme is available in Hurkmans et al. (2008), who recently developed the VIC model for the Rhine basin at a spatial resolution of 0.05×0.05 degree. The seven required atmospheric input time series are derived from a re-analysis dataset and are described in Section 2.4.1.

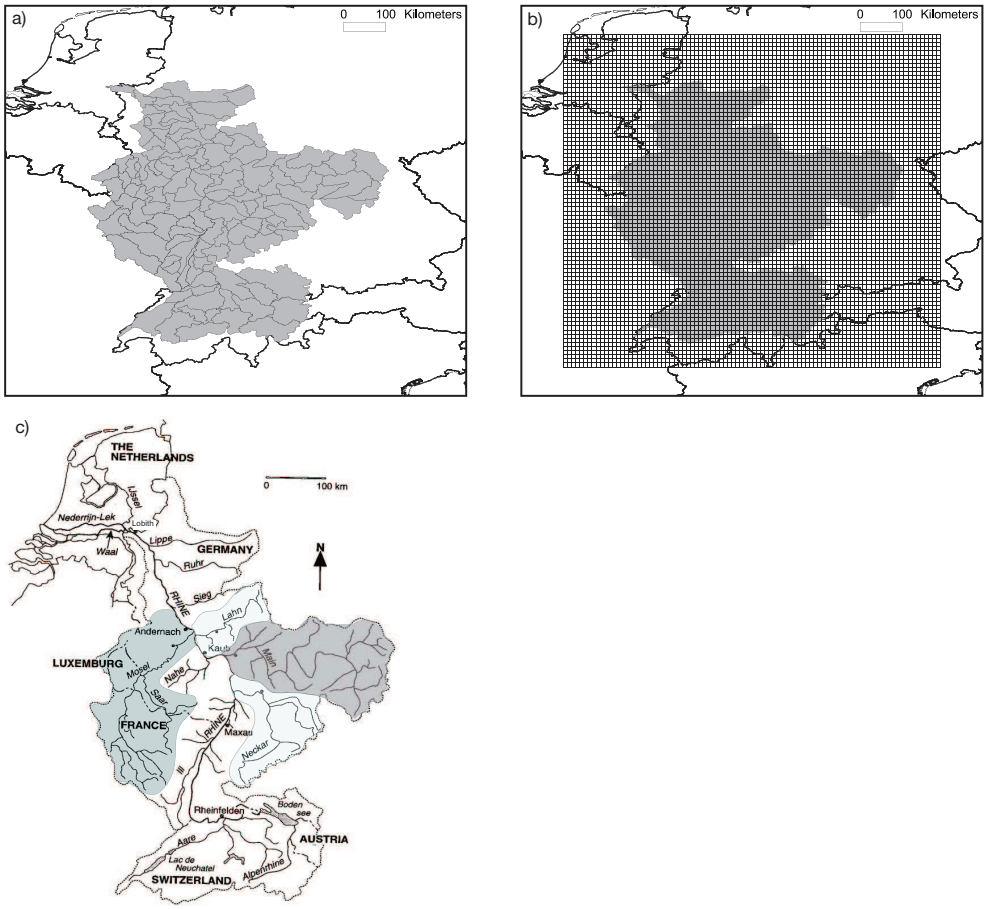

Figure 2.1: Map of the Rhine basin showing (a) 134 HBV sub-catchments; (b) the calculation grid used in VIC (0.05×0.05 degree); and (c) discharge measurement locations and sub-basins used in the analysis.

2.3.2 HBV

The HBV-96 model (Hydrologiska Byråns Vattenbalansavdelning) (Bergström, 1976; Lindström et al., 1997) model is a semi-distributed conceptual model. The model that is used in this study simulates discharge on a daily basis for 134 sub-basins of the Rhine. The model simulates snow accumulation, snowmelt, actual evapotranspiration, soil moisture storage, groundwater depth and runoff. The required forcing data are precipitation, temperature, and potential evaporation. The model consists of different routines in which snowmelt is computed by a day-degree relation, and groundwater recharge and actual evaporation are functions of actual water storage in a soil box. Discharge formation is represented by a linear reservoir for base flow and a non-linear approach for fast runoff components. Appendix A provides more information and an illustration of discharge formation in the HBV model. The sub-basins are linked together with a simplified Muskingum approach (Shaw, 2002) to simulate routing processes. The HBV model was developed for the Rhine in several steps since 1997 by the Dutch Institute for Inland Water Management and Waste Water Treatment (RIZA) and the German Federal Institute of Hydrology (BfG). A complete description of the HBV calculation scheme and the model structure for the Rhine basin is found in Eberle et al. (2005).

2.3.3 Rhine basin

The study area includes the Rhine basin (Figure 2.1) upstream of the Dutch-German border and covers an area of 160 800 km^2. The Rhine originates in the Alpine mountains that comprise almost 36 000 km^2 upstream of Basel, with maximum elevations of more than 4000 m a.s.l. Air temperatures are below zero during the winter season due to this height, and a substantial part of the precipitation is stored as snow. Land cover in the Alps is characterized by agricultural land in the lower regions and by forest, shrubs, meadows, unvegetated areas and glaciers on the higher slopes. The area of the Upper Rhine between Basel and Bingen is hilly, with elevations reaching over 1000 m a.s.l., but with flood plains along the main rivers. In the flood plains there is urban development, while the hills are mainly forested. The main tributaries Neckar, Main, Moselle, Lahn and Sieg have a mixed land use pattern, with agriculture and vineyards on the valley slopes, and forest on the hillslopes and mountains. The Middle Rhine has incised in higher grounds, which resulted in a deep narrow valley without floodplains. The relatively flat and low-lying Lower Rhine area downstream of Cologne until the Dutch-German border is an urbanized area with a mixture of agriculture, meadows and some forest. Overall, the Rhine basin is densely settled, with an average population density of 270 persons per km^2 (Early, 2001). About 50% of the basin is used for agriculture, 15–20% is urban or suburban land, and the remainder is forest and otherwise natural lands (Wessel, 1995).

Table 2.1: Basin and sub-basin characteristics. Surface area (km^2) is defined by the basin area upstream of the gauging station.

Basin	Gauge	Surface area (km^2)	Mean Q (m^3/s)	Min. Q (m^3/s)	Max. Q (m^3/s)	Mean ann. max. Q (m^3/s)	Data period
Rhine	Lobith	160 800	2 206	788	11 885	7473	1989–2005
Rhine	Andernach	139 549	2116	618	10 406	6494	1961–2004
Mosel	Cochem	27 088	334	10	4020	2190	1961–2004
Lahn	Kalkofen	5304	48	0	730	364	1961–2004
Main	Raunheim	27 142	176	44	1991	1043	1989–2005
Neckar	Rockenau	12 710	141	3	2105	1133	1971–1990
Rhine	Maxau	50 624	1297	379	4430	3191	1961–2004

The average discharge of the Rhine at Lobith is 2206 m^3/s (1989–1995). The mean annual maximum discharge is 7473 m^3/s, while the maximum discharge in the period since 1961 is 11 885 m^3/s, which occurred in January 1995 and caused floods in Germany. Parts of the Netherlands where evacuated, but against expectations the dikes held. Earlier considerable and some catastrophic floods in history are 1421, 1845, 1882 and 1926 (Disse and Engel, 2001). The surface area of the sub-basins under consideration in the present study vary from 5304 km^2 to 27 142 km^2, as can be seen from Table 2.1 among other basin characteristics.

2.4 Methods

2.4.1 Data

Both the HBV and VIC models were forced using downscaled ECMWF ERA15 atmospheric re-analysis data, which is provided by the Max Planck Institute for Meteorology (MPI), Hamburg, Germany. The regional climate model REMO (Jacob, 2001) was used for downscaling and this dataset will be further referred to as ERA15. The ERA15 data set comprises the years 1993 through 2003, at a 3-hourly time step, with a grid resolution of 0.088 degrees and provides the following forcing data: precipitation, temperature, specific humidity, air pressure, downward radiation (shortwave and longwave) and wind speed. These input data are all required to run the VIC model.

To compare this data to observations, two additional meteorological datasets are available. First, a historical data set is available from the International Commission for the Hydrology of the Rhine basin (CHR). This data set is referred to as CHR and contains daily values of precipitation and temperature for the years 1961 through 1995, which are based on 36 measurement stations throughout the basin (Sprokkereef,

2001). Second, a historical dataset using interpolated measured data is available from the Climate Research Unit (CRU) where they develop a number of global datasets widely used in climatic research. This data set is referred to as CRU (Mitchell and Jones, 2005) and contains precipitation and temperature values at a monthly time step and comprises the years 1900 through 1998, with a grid resolution of 0.5 degrees.

HBV was also forced by CHR precipitation and temperature data and VIC only by CHR precipitation. VIC could not be forced by CHR temperature, because the models needs daily variation of temperature and therefore requires 3 or 6 hourly values of minimum and maximum temperature data. HBV only needs daily values of these forcing parameters, and at least monthly mean values of potential evaporation as input data. As a consequence of the detailed data input requirements of the VIC model, the ERA15 data still provided the remaining forcing parameters in combination with the CHR precipitation values. Combining measured values with RCM output data disturbs the water balance of the RCM output. It creates a figurative, but false forcing data set. Precipitation values of the CRU data set were only used for comparison of forcing data.

Additional spatial information on altitude, soil types and land cover is derived from a GIS database available at Federal Institute of Hydrology in Germany (Eberle et al., 2005). Historical discharge data was provided by the Dutch governmental Institute for Inland Water Management and Waste Water Treatment (RIZA).

2.4.2 Forcing data comparison

Rainfall amounts of the three forcing datasets were compared for the period of 1993–1995; the only three years the three datasets all overlap. A first comparison was made for basin wide mean values at a daily basis between the ERA15 and CHR values. For the second comparison, the ERA15 and CHR data sets were aggregated to weekly and monthly values and then compared to the CRU data.

2.4.3 Model performance

Calibration at Lobith

As is explained in Section 2.4.1, HBV and VIC were forced both by ERA15 and CHR precipitation values for comparison reasons. For VIC this results in a forcing data set containing a combination of measured data for precipitation and RCM output for the remaining seven input parameters. This forcing dataset is considered incorrect and therefore both models were calibrated using only ERA15 output.

Table 2.2: Performance criteria daily and monthly discharge values at Lobith for the calibration period (March 1993–December 1993) and the validation period (1994–2003).

		Calibration period		Validation period	
		daily	monthly	daily	monthly
E	VIC ERA15	0.47	0.26	0.31	0.40
	HBV ERA15	0.49	−0.08	0.62	0.60
	VIC CHR	0.44	0.35	–	–
	HBV CHR	0.85	0.73	–	–
r^2	VIC ERA15	0.64	0.58	0.54	0.67
	HBV ERA15	0.75	0.54	0.65	0.64
	VIC CHR	0.81	0.88	–	–
	HBV CHR	0.97	0.96	–	–
VE	VIC ERA15	0.23	0.23	0.08	0.08
	HBV ERA15	0.32	0.32	−0.04	−0.04
	VIC CHR	−0.55	−0.55	–	–
	HBV CHR	0.19	0.19	–	–

We forced both models with ERA15 data and calibrated for the discharge gauge at the Dutch-German border at Lobith (see Figure 2.1c) using observed discharge at Lobith for the year 1993. Only one year was used in order to limit the amount of calibration time for the VIC model. Because 1993 contains a relatively dry summer, as well as an extreme peak in winter, it was considered representative of the extremes for the total period. The model simulations were initialized using model states of October 1993 and also the first two months of 1993 are considered as a 'warm-up' period, hence model results for this period were not used in the calibration process.

To calibrate VIC, former applications of VIC (Liang et al., 1994) were followed in that seven parameters were selected for calibration using an automated approach. These seven parameters describe the layer depths, relations between soil moisture content and baseflow and the infiltration capacity. For a complete description, see Hurkmans et al. (2008).

The original calibration process for the HBV model of the Rhine basin is described by Eberle et al. (2005). HBV was recalibrated for the year 1993 in a stepwise approach using the ERA15 dataset. Based on results of a parameter sensitivity analysis by Passchier and Stone (2003), for HBV, only the parameters *fc* (field capacity that represents the total water storage capacity of the soil) and *khq* (describing the quick runoff function) were adjusted for recalibration.

Sub-basin scale validation performance

The calibrated models are validated using the remaining period of the ERA15 data set, the years 1994 through 2003. There is a large number of efficiency criteria to choose from for model validation, such as those presented by Krause et al. (2005) and each criterion may place different emphasis on different types of simulated and observed behaviors. The objective performance criteria used in the current study to compare the integral time series for the locations, are the coefficient of efficiency (E) (Nash and Sutcliffe, 1970), the coefficient of determination (r^2) and the volume error (VE). For a description of these performance criteria, see Appendix D.

Model performance differs with the scale on which it is applied. In the present study we are interested in discharges at Lobith (the outlet of the basin), discharges upstream in the main Rhine channel and model performance at the sub-basin scale. The discharge gauges that were used in the analysis are Lobith, Andernach and Maxau along the Rhine branch, and tributary gauging stations at Cochem (Moselle), Kalkofen (Lahn), Raunheim (Main) and Rockenau (Neckar). These locations are shown in Figure 2.1 and characteristics of the sub-basins upstream of those gauges are presented in Table 2.1.

Peak flows and low flows

Periods with extreme discharges are often of most interest both in impact studies and real time flow predictions. A good representation by the model of the absolute amount, the timing and duration of the peak and low flows is very relevant. Subsequently, just for the gauge at Lobith, we selected five peak flow and five low flow periods, and chose additional performance indicators that relate to magnitude and timing of peak flows, together with minimum values and duration of low flows. These indicators are observed maximum discharge (max. Q_{obs}), relative difference between observed and simulated maximum discharge ($d$max. Q_{sim}), difference in peak timing (dT), observed minimum discharge (min. Q_{obs}), relative difference between observed and simulated minimum discharge ($d$min. Q_{sim}) and duration of the low flow period under a threshold of $1300\,\mathrm{m}^3/\mathrm{s}$ (DUT). A discharge of $1300\,\mathrm{m}^3/\mathrm{s}$ at Lobith is a critical value in summer periods; lower discharges affect shipping industry, agricultural supply, electricity production and drinking water supplies.

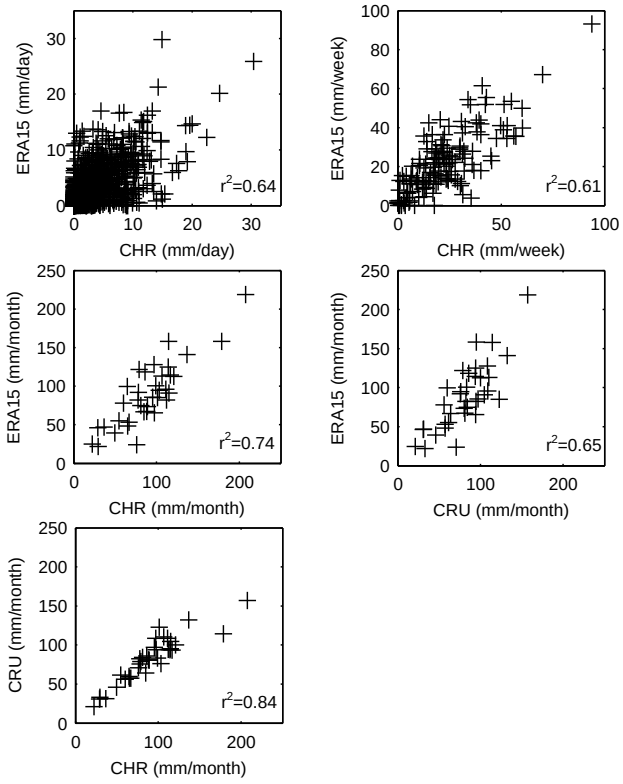

Figure 2.2: ERA15 versus CHR versus CRU precipitation. The period 1993–1995 was used for the comparison.

2.5 Results

2.5.1 Forcing data comparison

The difference between measured precipitation data (CHR and CRU) and reanalysis data (ERA15) provides an indication for the error or bias in the reanalysis data set. The assumption here is that measured data better represents actual values than reanalysis data and to test this assumption both measured datasets are compared with ERA15 data. Figure 2.2 illustrates the correlation between the precipitation data at different time steps. Daily values of ERA15 and CHR correlate poorly (r^2=0.41) while the correlation coefficient increases with increasing time step length. The precipitation values of the ERA15 data do not show a constant bias that can be corrected. The correlation between monthly values of ERA15 and CHR is reasonably well (r^2=0.74) and slightly higher than between ERA15 and CRU (r^2=0.65). The correlation between CHR and CRU, however, has an r^2 value of 0.84, which indicates that these two databases are most alike and that ERA15 probably has a larger error than the measured data.

2.5.2 Model performance

Calibration and validation period at Lobith

Daily values of all performance criteria for Lobith are displayed in Table 2.2, where a distinction is made between the calibration and the validation period. The additional six locations will be discussed below. At Lobith after calibration, the results of the HBV model forced with ERA15 show a moderate performance (E=0.49, r^2=0.75), whereas the VIC model fits less well (E=0.47, r^2=0.64). This is mainly caused by an overestimation of the volume, by 23% (VIC) and 32% (HBV), respectively. VIC forced by CHR shows an increased correlation (r^2=0.81) when compared to its performance when forced by ERA15, but a decrease on the other performance criteria (E=0.44, VE=−0.55). However, the HBV model forced with CHR fits well when compared to observed discharges (E=0.85, r^2=0.97).

Figure 2.4 depicts the results of the period 1993–2003 at Lobith, respectively for the VIC and the HBV models both forced with ERA15 data. The HBV model shows a better fit of the simulated discharge to the observed discharge than VIC, which is confirmed by the efficiency coefficients as shown in Table 2.2. The coefficient of efficiency (E) of HBV is 0.62, where VIC shows 0.31 and coefficient of determination (r^2) of HBV is 0.65, where VIC displays 0.54. The volume error of both models is low (−4% by HBV and 8% by VIC). A visual analysis of the hydrographs at multiple peak flow events, shows that both models simulate the recession curve well. Errors arise

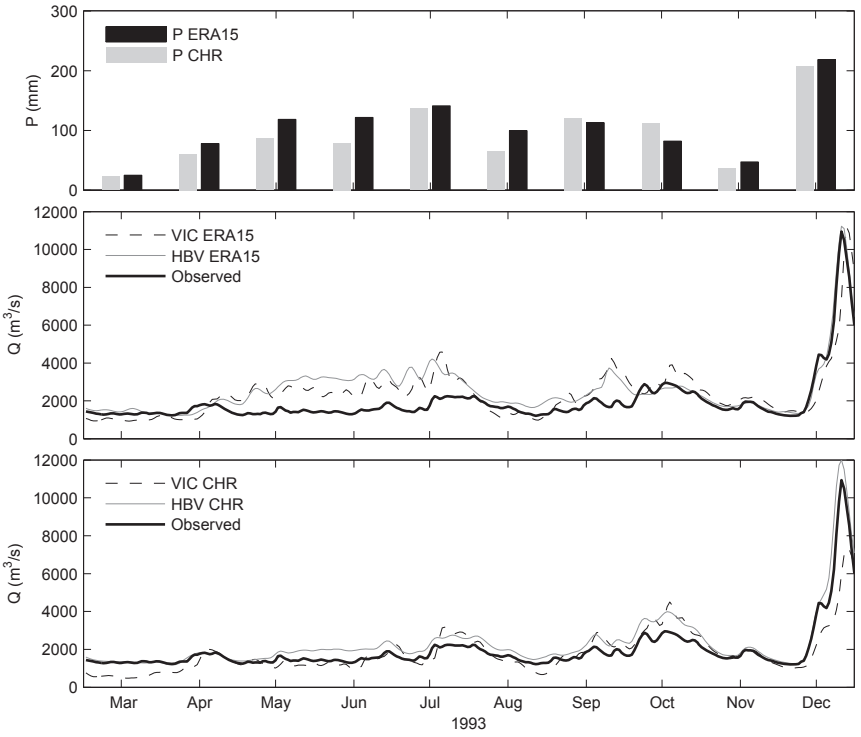

Figure 2.3: Monthly precipitation values for the Rhine basin according to different datasets (top) and daily discharge values at Lobith (bottom); model simulation results for the calibration period compared to the observed discharge in the period March–December 1993.

at most extreme peak events (see section below) on peak flows and low flows) where the quick flow component either is too small or too large. VIC tends to overestimate more peaks than HBV does and shows a delayed peak at many peak events. Medium flows are mostly well represented by HBV, whereas VIC substantial over estimates discharges, sometimes for a period of several months. Low flow periods are simulated well for a length of time up to 2 or 3 months, and when drought periods are more lengthy, both models tend to underestimate baseflow. The changeable reaction of both models to different meteorological conditions suggests that the storage capacity in the upper layers is very irregular, resulting in variable estimates of direct runoff. Also, the depletion factor controlling drainage from the lower layers seems to be too large during lengthy drought events.

A further explanation for these moderately successful results might be that at a short time step like a daily basis, errors in timing of simulated high and low flows have a considerable negative influence on the performance indicators. Nonetheless, when

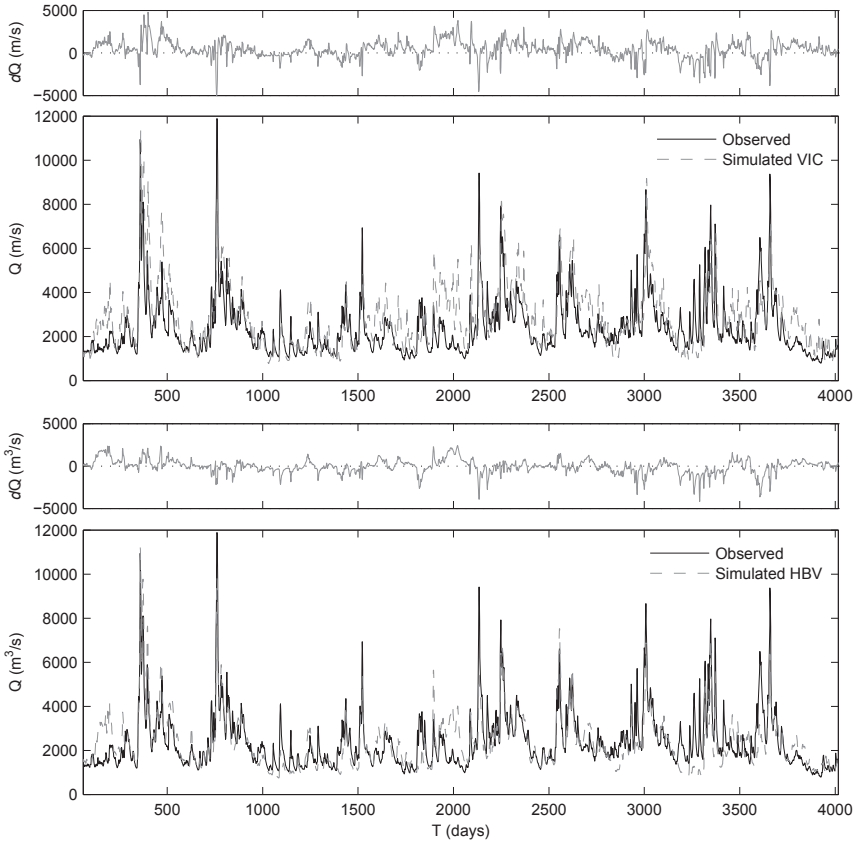

Figure 2.4: Daily simulation results of the HBV model (a) and the VIC model (b) compared to the observed river discharge for the period 1993–2003 (4017 days).

Table 2.3: Observed and simulated mean, minimum and maximum discharge (in m^3/s), their standard deviation (SD) and skewness for the period March 1993 through December 2003.

Basin	Gauge		Mean Q (m^3/s)	Min Q (m^3/s)	Max Q (m^3/s)	SD (m^3/s)	Skewness (–)
Rhine	Lobith	Observed	2387	788	11 885	1300	2.29
		VIC	2811	773	11 394	1468	1.45
		HBV	2339	746	11 228	1244	1.99
Rhine	Andernach	Observed	2197	630	10 500	1182	2.29
		VIC	2474	734	10 487	1258	1.46
		HBV	2054	593	11 092	1104	2.08
Mosel	Cochem	Observed	355	31	4020	416	3.20
		VIC	325	49	2463	282	2.63
		HBV	263	21	3644	274	4.37
Lahn	Kalkofen	Observed	48	0	598	61	3.86
		VIC	42	6	350	42	2.44
		HBV	33	1	506	40	4.21
Main	Raunheim	Observed	183	51	1,991	197	3.65
		VIC	234	39	1885	227	2.48
		HBV	180	44	1946	189	3.89
Neckar	Rockenau	Observed	150	27	2140	142	5.26
		VIC	216	34	2490	201	3.17
		HBV	144	19	2291	167	4.93
Rhine	Maxau	Observed	1322	400	4330	530	1.38
		VIC	1631	374	5222	739	0.98
		HBV	1335	407	5137	629	1.18

monthly values of simulated discharge are evaluated they display similar or slightly worse results, as can be seen from Table 2.2; VIC and HBV forced with ERA15 perform moderately and HBV forced with CHR fits well, which is about equal to the HBV simulations at a daily basis. The difference in coefficient of efficiency (E) between daily and monthly values of the HBV model forced with ERA15 in the calibration period stands out though, a moderate 0.49 for daily values and a dramatic -0.08 for monthly values. Instead of the expected damping effect on performance, aggregating to a bigger time step indeed causes the observed and modeled peak value of several days in December 1993 (shown in Figure 2.3) to damp, but does not effect the more or less consistent over estimation during the months May until July. Since the coefficient of efficiency (E) is sensitive to peak values, in this case the absolute observed and modeled discharge values are damped, but the relative error by time step increases which causes the coefficient to drop.

These results indicate that forcing data largely influence the performance values of both models. A closer examination of the precipitation values in both forcing data sets during the calibration period is depicted in Figure 2.3, together with observed

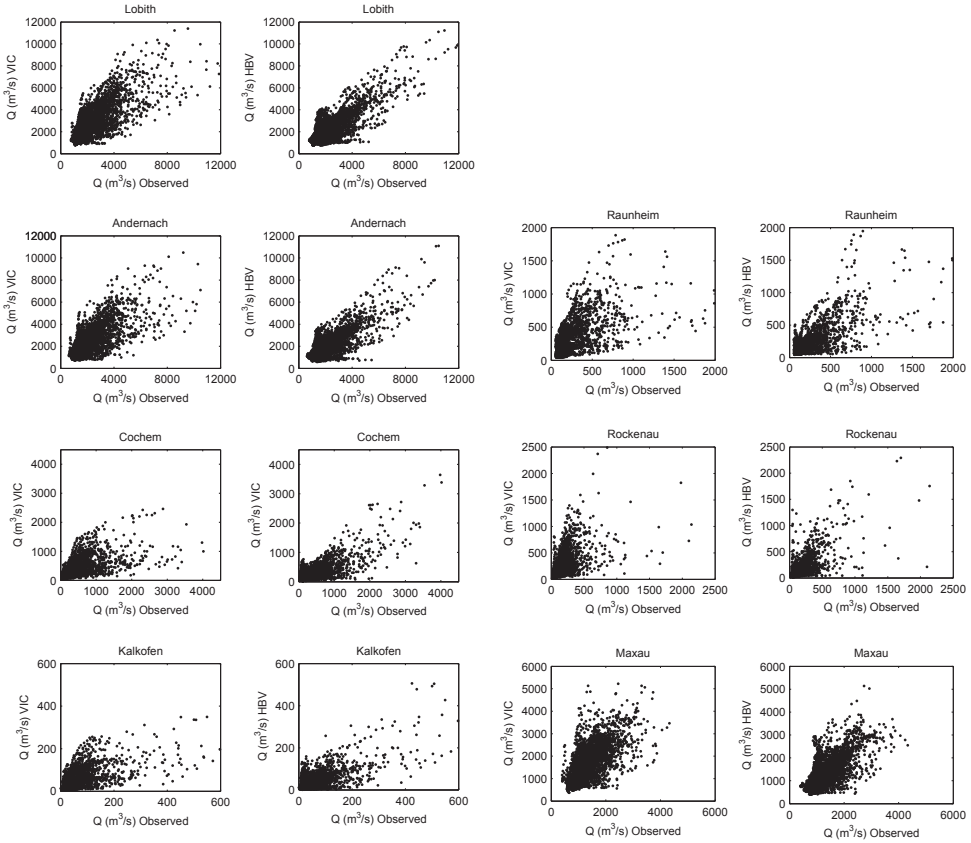

Figure 2.5: Scatter plots of observed and simulated discharge Q (m^3/s) at a daily basis. The results for VIC are displayed on the left side and for HBV on the right side.

and simulated discharge values. The figure shows that during the months May, June and July, both HBV and VIC forced with ERA 15 consistently overestimate discharge by 25–100%, whereas HBV forced with CHR also overestimates discharge, but to a lesser degree. VIC forced by CHR shows an even better fit for these months. This can be explained by the equally consistent higher ERA15 precipitation values when compared to the CHR data. In August, ERA15 again displays higher values than the CHR data, while observed and simulated discharge agree quite well. This lack of reaction in modeled discharge in August can be explained by higher evaporation values during summer than spring, which neutralize the precipitation surplus, next to the fact that absolute precipitation values are lower in summer than in springtime.

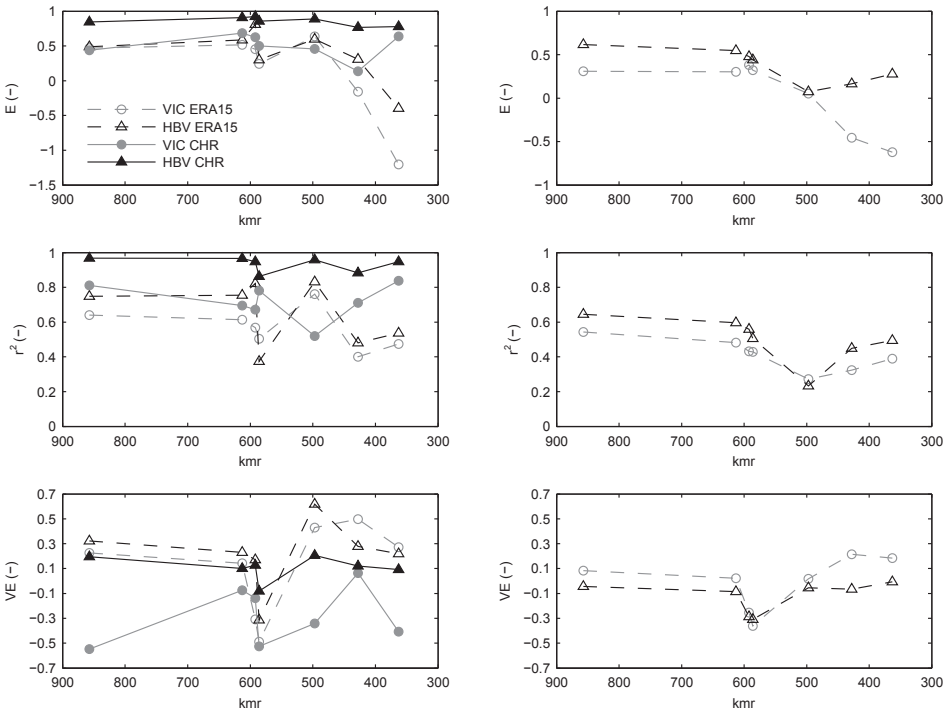

Figure 2.6: Performance criteria daily discharge values. *kmr* represents the length of the Rhine from the Bodensee. The calibration period is displayed at the left side and the validation period at the right side.

Sub-basin scale performance

Several statistical parameters for the complete simulation period are presented in Table 2.3. The mean and minimum simulated discharges agree reasonable well for the HBV model, whereas VIC overestimates those values, except for the gauges at Cochem and Kalkofen. The maximum discharges, though, are underestimated for most locations, except for the most upstream gauges Rockenau and Maxau. The values for the standard deviation (SD) based on daily values are high for both simulated and observed values. This can be explained by the skewed distribution of the discharge values. Based on this information it can be concluded that the probability density function of the observed values at Lobith is best represented by the simulated discharges by HBV.

For the remaining six gauges upstream of Lobith, scatter plots of the daily observed and simulated discharges are displayed (Figure 2.5) for the validation period. The

Table 2.4: Performance criteria daily discharge values. *kmr* represents the length of the Rhine from the Bodensee.

Calibration period								
	kmr	857	613	592	586	497	428	363
		Lobith	Andernach	Cochem	Kalkofen	Raunheim	Rockenau	Maxau
E	VIC ERA15	0.47	0.52	0.45	0.24	0.64	−0.16	−1.20
	HBV ERA15	0.49	0.59	0.81	0.30	0.60	0.31	−0.40
	VIC CHR	0.44	0.68	0.63	0.50	0.46	0.14	0.64
	HBV CHR	0.85	0.91	0.92	0.86	0.89	0.77	0.78
r^2	VIC ERA15	0.64	0.61	0.57	0.50	0.76	0.40	0.47
	HBV ERA15	0.75	0.75	0.82	0.37	0.83	0.48	0.54
	VIC CHR	0.81	0.81	0.69	0.67	0.78	0.52	0.71
	HBV CHR	0.97	0.97	0.95	0.86	0.96	0.88	0.95
VE	VIC ERA15	0.23	0.14	−0.31	−0.49	0.43	0.50	0.27
	HBV ERA15	0.32	0.23	0.17	−0.31	0.62	0.28	0.22
	VIC CHR	−0.55	−0.07	−0.14	−0.52	−0.34	0.06	−0.41
	HBV CHR	0.19	0.10	0.13	−0.08	0.21	0.12	0.09
Validation period								
	kmr	857	613	592	586	497	428	363
		Lobith	Andernach	Cochem	Kalkofen	Raunheim	Rockenau	Maxau
E	VIC ERA15	0.31	0.30	0.38	0.32	0.05	−0.46	−0.62
	HBV ERA15	0.62	0.55	0.48	0.44	0.07	0.17	0.28
r^2	VIC ERA15	0.54	0.48	0.43	0.43	0.27	0.32	0.39
	HBV ERA15	0.65	0.60	0.56	0.51	0.23	0.45	0.49
VE	VIC ERA15	0.08	0.02	−0.25	−0.36	0.02	0.21	0.18
	HBV ERA15	−0.04	−0.09	−0.29	−0.31	−0.05	−0.07	−0.01

accessory r^2 values are presented in Table 2.4. Table 2.4 and 2.5 show the results of all performance criteria for daily and monthly values respectively, for all locations. Above the location name, the *kmr* number is displayed. This number represents the length of the Rhine from the Bodensee in Switzerland and Germany. For example, the gauging station at Lobith is located 857 km downstream form the Bodensee. In the current study, the gauges that are not located exactly along the Rhine, but along tributaries draining the sub-basins, have *kmr* numbers that represent locations where the side rivers enter the Rhine. The *kmr* number is used to illustrate all performance criteria as presented in Table 2.4 and 2.5, in a graphical way in Figure 2.6 and Figure 2.7. In Figure 2.7, the volume error is not displayed, since the volume error does not change when the time step is adjusted (see Table 2.4 and 2.5).

The Nash & Sutcliffe efficiency coefficient (E) decreases in the upstream direction, sometimes even below zero at Rockenau and Maxau for VIC results. An efficiency lower than zero indicates that the mean value of the observed time series would have been a better predictor than the model. From all graphs on the left side representing the calibration period, it is obvious that HBV forced with CHR performs considerably better than VIC forced with CHR and than both models forced with ERA15. Nonetheless, VIC forced with CHR performs better than VIC forced with ERA15, especially in upstream direction. Moreover, for the ERA15 forcing, HBV performs

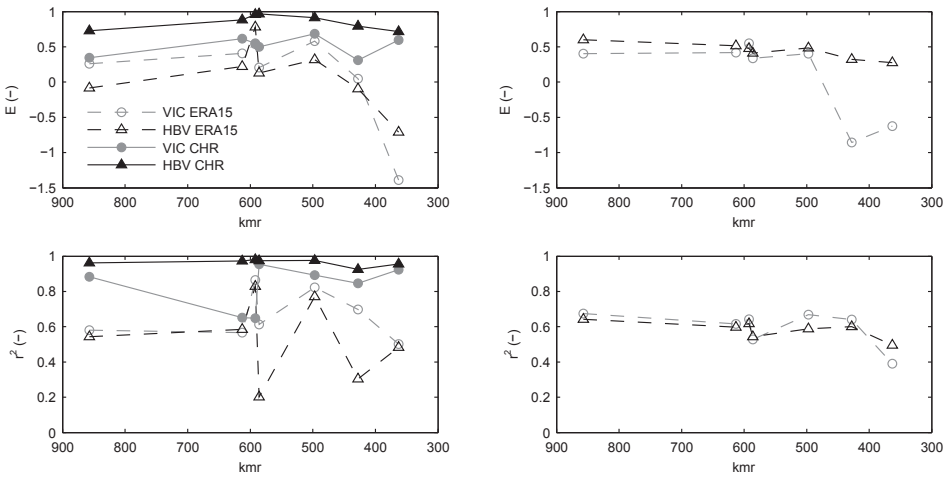

Figure 2.7: Performance criteria monthly discharge values. *kmr* represents the length of the Rhine from the Bodensee. The calibration period is displayed at the left side and the validation period at the right side.

marginally better than VIC at a daily basis, whereas VIC performs marginally better than HBV at a monthly basis. When studying the validation period on the right side, however, HBV performs substantially better than VIC, which indicates that HBV is more robust in its performance.

Peak flows and low flows

Table 2.6 shows the five highest daily discharges and the five lowest monthly discharges, as observed and simulated at Lobith. Observed volumes over threshold and maximum peak discharges reveal that both models overestimate and underestimate the same peaks. Furthermore, it shows that VIC tends to delay flood peaks, for some peaks even up to 6 days, while HBV simulates the timing of the peaks very well. Two factors in VIC explain this delaying of peak flows: first, the routing algorithm that is used in VIC might delay arrival at Lobith slightly compared to the internal routing algorithm in HBV. This was also noted in Hurkmans et al. (2008) where runoff from another conceptual water balance model (STREAM) was routed with different algorithms. Second, the degree to which peaks are delayed also depends on calibration parameters, particularly depths of the upper layers and the infiltration capacity factor (see for details on VIC calibration Hurkmans et al. (2008)). When the resulting infiltration capacity is higher, there is less direct runoff and, in case of near-saturation, excess water is, with a small delay, transported as baseflow. For the peak of 1993, which is included in the calibration period, the simulated timing by VIC was rather

Table 2.5: Performance criteria monthly discharge values. *kmr* Represents the length of the Rhine from the Bodensee.

Calibration period								
	kmr	857	613	592	586	497	428	363
		Lobith	Andernach	Cochem	Kalkofen	Raunheim	Rockenau	Maxau
E	VIC ERA15	0.26	0.41	0.54	0.21	0.58	0.05	−1.39
	HBV ERA15	−0.08	0.22	0.78	0.13	0.32	−0.09	−0.71
	VIC CHR	0.35	0.61	0.55	0.50	0.68	0.31	0.59
	HBV CHR	0.73	0.88	0.96	0.97	0.91	0.79	0.72
r^2	VIC ERA15	0.58	0.57	0.86	0.61	0.82	0.70	0.50
	HBV ERA15	0.54	0.58	0.83	0.20	0.77	0.30	0.48
	VIC CHR	0.88	0.65	0.65	0.95	0.89	0.85	0.92
	HBV CHR	0.96	0.97	0.98	0.97	0.98	0.93	0.96
VE	VIC ERA15	0.23	0.14	−0.31	−0.49	0.43	0.50	0.27
	HBV ERA15	0.32	0.23	0.17	−0.31	0.62	0.28	0.22
	VIC CHR	−0.55	−0.07	−0.14	−0.52	−0.34	0.06	−0.41
	HBV CHR	0.19	0.10	0.13	−0.08	0.21	0.12	0.09
Validation period								
	kmr	857	613	592	586	497	428	363
		Lobith	Andernach	Cochem	Kalkofen	Raunheim	Rockenau	Maxau
E	VIC ERA15	0.40	0.42	0.55	0.34	0.40	−0.86	−0.62
	HBV ERA15	0.60	0.52	0.48	0.41	0.48	0.32	0.28
r^2	VIC ERA15	0.67	0.62	0.64	0.53	0.67	0.64	0.39
	HBV ERA15	0.64	0.60	0.62	0.54	0.59	0.60	0.49
VE	VIC ERA15	0.08	0.02	−0.25	−0.36	−0.03	0.22	0.18
	HBV ERA15	−0.04	−0.09	−0.29	−0.31	−0.09	−0.06	−0.01

accurate, however, for other peaks in the validation period these parameter settings were apparently less applicable.

Concerning the low flows, VIC tends to underestimate the minimum values and HBV tends to overestimate the low flows under consideration. For the duration of the most extreme low flows below a threshold of $1300\,\mathrm{m}^3/\mathrm{s}$, both models underestimated the duration of the low flows significantly and showed variable performance on the less extreme low flow periods.

2.6 Discussion and conclusions

In the view of the utility of hydrological models in climate scenario studies, the goal of this Chapter was to compare the hydrological models HBV and VIC by testing their performance for simulating historical discharge in the Rhine basin. These models have different model structures and there is no consensus in research on rainfall-runoff modeling on what model structure is to be preferred. Some research suggest, however, that the VIC approach more accurately simulates the timing of peak discharges (Troy et al., 2007). Different meteorological data sets were used as model input and HBV

Table 2.6: Analysis of peak flows and low flows at the outlet of the basin (Lobith), showing observed maximum discharge (max. Q_{obs}), relative difference between observed and simulated maximum discharge ($d$max. Q_{sim}), difference in peak timing (dT), observed minimum discharge (min. Q_{obs}), relative difference between observed and simulated minimum discharge ($d$max. Q_{sim}) and duration of the low flow period under a threshold of 1300 m^3/s (DUT).

Peak flows	31/01/1995	25/12/1993	04/11/1998	07/01/2003	28/03/2001
Max. Q_{obs} (m^3/s)	11 775	11 034	8410	9366	8666
$d$max. Q_{sim} VIC (%)	−26.7	1.5	−35.1	−15.5	−12.5
$d$max. Q_{sim} HBV (%)	−16.3	0.9	−34.9	−32.1	−20.6
dT VIC (days)	2	2	6	5	4
dT HBV (days)	0	0	0	−1	−1

Low flows	09/2003	11/1997	08/1998	09/1996	03/1993
Min. Q_{obs} (m^3/s)	788	931	983	1077	1228
$d$min. Q_{sim} VIC (%)	−20.3	−10.7	4.5	−26.0	−38.5
$d$min. Q_{sim} HBV (%)	18.7	6.5	44.4	−15.8	0.5
DUT Q_{obs} (days)	141	68	39	37	13
DUT VIC (days)	104	22	15	60	68
DUT HBV (days)	93	33	0	54	11

and VIC were compared at both basin and sub-basin scale using various performance criteria. Furthermore, simulated peak flows and low flows were compared.

We have seen that the performance of both models was less in upstream basins than at the basin outlet (gauging station Lobith), but that for all upstream basins HBV still performed better than VIC at a daily basis. We have seen that HBV was more robust when the performance of the calibration period (E=0.49, r^2=0.75 vs. E=0.47, r^2=0.64 at Lobith) and the validation period (E=0.62, r^2=0.65 vs. E=0.31, r^2=0.54 at Lobith) were compared. In addition, HBV forced with CHR data (E=0.85, r^2=0.97 for the calibration period at Lobith) performed much better than VIC forced with CHR (E=0.44, r^2=0.81) and than both VIC and HBV forced with ERA15.

For the most extreme peak flows, HBV simulated maximum discharges best ($d$max. Q_{sim} HBV 1–17%, $d$max. Q_{sim} VIC 2–27%), while VIC performed better at the moderate peak flows ($d$max. Q_{sim} HBV 21–35%, $d$max. Q_{sim} VIC 13–35%). Besides simulating measured values of discharges, timing of peak flows was investigated. It appeared that VIC displayed several days delay in estimating timing of the peak discharge. Most low flows were underestimated by VIC, where HBV showed overestimation of the low flows. Also the performance of both models in reproducing duration of low flows was poor.

Hence, the semi-distributed lumped conceptual HBV model performed much better than the distributed land surface model VIC. This deflects from the general idea that

more complex distributed modeling better represents observed discharges as compared to simple conceptual model approaches (Refsgaard, 1996; Reggiani and Schellekens, 2003). These results support the notion that even for a well documented river basin such as the Rhine, more complex modeling does not automatically lead to better results (Booij, 2003; Uhlenbrook, 2003).

We are convinced, though, that VIC should be able to perform better than it has done so far in the Rhine basin, and thus model performance might be improved (Hurkmans et al., 2008). The performance of VIC might increase using a longer calibration period and further refining the spatial distribution of adjusted parameters. Furthermore, by solving both the water and the energy balance VIC holds the potential to better describe soil-atmosphere feedback processes, if the model scheme were to be combined with an atmospheric model. In the line of small-scale hydro-meteorology and modeling the effects of land use change, this is a conclusive reason for further development (Hurkmans et al., 2008). Moreover, VIC has performed well in the past, for example in studies by Liang et al. (1994) and Troy et al. (2007). But also the HBV model for the Rhine basin can be improved. Lake retention for example, is not implemented yet in both models. Especially concerning the Bodensee, a large upstream lake in the Rhine basin, this is a quite drastic simplification and an obvious potential for further improvement. We subscribe the recommendation of (Seibert, 1999), that model development and calibration is an undertaking that should not be carried out by a single researcher, but requires scientific dialog.

The results also lead us to the conclusion that forcing data has a considerable influence on model performance, irrespectively to the type of model structure. It emphasizes the need for ground-based meteorological measurements and a suggestion might be to correct downscaled climate model re-analysis data such as ERA15, whenever measurements are available. It should be kept in mind that comparing mean values of precipitation and temperature provides little guide to the quality of the data during more extreme events that affect hydrological systems. Pitman and Perkins (2007), for example, propose a probability density function based assessment and a skill score that shows a climate model's ability to simulate the 95^{th} rainfall percentile. Comprehensive comparison and correction of downscaled climate model output is a challenging task for further research.

The conclusion as to the application of hydrological models in climate scenario studies, then, is that for the Rhine basin HBV is preferred, since it has shown better overall performance and seems to be more robust than VIC. The extreme events were simulated best by HBV, which implies that HBV can provide the most reliable indication of possible future shifts in extreme events due to climate change. The more realistic representation of evaporation processes by VIC than HBV did not result in better performance even in the dry periods, when the evaporation volume is substantial in the water balance. The final advantage of HBV over VIC is that HBV has

short computation times, which makes it suitable for simulating long time series of the many available different climate scenarios.

Acknowledgements

This research was supported by the project ACER (A7) under the Dutch BSIK Climate Changes Spatial Planning program. We wish to thank H. Buiteveld from the Dutch Institute for Inland Water Management and Waste Water Treatment (RIZA) and the German Federal Institute of Hydrology (BfG) for both allowing the use of the HBV model, and providing meteorological and discharge measurement data. D. Jacob and E. Mazurkewitz from the Max Planck Institute for Meteorology are kindly acknowledged for providing meteorological data. Finally we thank two anonymous colleagues for occasional data editing and their constructive comments that helped to improve this Chapter.

Chapter 3

Simulating low probability peak discharges using resampled climate modeling data

Te Linde, A.H., Aerts, J.C.J.H., Bakker, A.M.R. and Kwadijk, J.C.J., 2010. Simulating low probability peak discharges for the Rhine basin using resampled climate modeling data. *Water Resources Research*, 46 (WR03512), doi: 10.1029/2009WR007707.

Abstract

Climate change will increase winter precipitation and in combination with earlier snowmelt it will cause a shift in peak discharge in the Rhine basin from spring to winter. This will probably lead to an increase in the frequency and magnitude of extreme floods. In this Chapter we aim to enhance the simulation of future low probability flood-peak events in the Rhine basin using different climate change scenarios and downscaling methods. We use the output of a regional climate model (RCM) and a weather generator to create long, resampled time series (1000 years) of climate change scenarios as input for hydrological (daily) and hydrodynamic (hourly) modeling. We applied this approach to three parallel modeling chains, where the transformation method from different resampled RCM outputs to the hydrological model varied (delta change approach, direct output, and bias-corrected output). On the basis of numerous 1000-year model simulations the results indicate a basin-wide increase in peak discharge in 2050 of 8% to 17% for probabilities between 1/10 and

1/1250 years. Furthermore, the results show that increasing the length of the climate data series using a weather generator reduced the statistical uncertainty when estimating low probability flood-peak events from 13% to 3%. We further conclude that bias-corrected direct RCM output is to be preferred over the delta change approach, because it provides insight in geographical differences in discharge projections under climate change. Also, bias-corrected RCM output can simulate changes in the variance of temperature and rainfall and in the number of precipitation days, as changes in temporal structure are expected under climate change. These added values are of major importance when identifying future problem areas due to climate change, and when planning potential adaptation measures.

3.1 Introduction

Recent research findings conclude that climate change will increase the risk of flooding around the world (Milly et al., 2002, 2005; IPCC, 2007a). In North-West Europe, both observations and models agree on a trend towards wetter winter conditions (EEA, 2008). In the Rhine basin, the peak discharge is likely to move from spring to winter in many areas due to earlier snowmelt in addition to increased precipitation in winter (e.g. Middelkoop et al., 2001; Kundzewicz et al., 2007). This will probably lead to an increase in flood frequency (Hooijer et al., 2004; Pinter et al., 2006).

As extreme discharge events are more important in water management than mean values, estimates of changes in the frequency and magnitude of floods are desired for the planning of adaptation measures. For estimating future flood frequencies, climate change scenarios are used as input for hydrological models. For sub-continental basins like the Rhine, however, the spatial resolution of a general circulation model (GCM) is inadequate for forcing a hydrological model and downscaling is required. This can be done by means of perturbation of historical series with average changes of climate parameters, referred to as the delta change approach (Lenderink et al., 2007a; Te Linde, 2007), by means of statistical downscaling (Jacob et al., 2008), or by dynamic downscaling using regional climate models (RCMs) that are nested in a GCM (Kay et al., 2006). The latter is known as the direct forcing approach. This is an emerging field as climate models continue to improve, and different methods are available to downscale and transform climate change scenarios for hydrological modeling studies (Wilby et al., 2000; Menzel et al., 2006; Lenderink et al., 2007b). All methods result in future meteorological time series that are used as input in hydrological models to simulate the hydrological response to climate forcing. The resulting discharge series can then be used to estimate future flood-peak probabilities.

The estimation of probabilities of very rare extreme events ($> Q_{200}$, i.e. a discharge with a return period longer than 200 years), however, is far from trivial. For the

present conditions, frequency analysis is often applied on historical discharge series, which requires the extrapolation of fitted extreme value distributions (Kottegoda, 1980; Garrett and Müller, 2008). Safety levels along the Rhine are relatively high, up to 1/1250 per year at Lobith, and with $\sim$110 years observed discharge data available, statistical extrapolation leads to very large uncertainties (Klemeš, 2000a,b). More sophisticated approaches combine weather generators with hydrological models (Buishand and Brandsma, 2001; Orlowsky et al., 2007) to create such long discharge series that extrapolation is redundant. This approach is also not without debate, since it requires hydrological modeling of extreme events far beyond historic event size.

Earlier hydrological studies on the effects of climate change on peak discharges in the Rhine basin revealed that mean winter discharges are expected to increase by 5–30% and mean summer discharge to decrease by 0–45% by 2050 (compared to the current climate), using a range of climate change scenarios, from different GCMs, RCMs, and hydrological modeling methods (Buishand and Lenderink, 2004; Hundecha and Bárdossy, 2005; Fujihara et al., 2008). As a consequence, the once in 1250-year flood event at the gauging station of Lobith (which is the current design discharge at the border of Germany and the Netherlands) is estimated to increase from 16 000 m^3/s at present to somewhere between 16 500 and 19 500 m^3/s in 2050 (Kwadijk and Middelkoop, 1994; Grabs, 1997; Shabalova et al., 2003; Lenderink et al., 2007a). A shortcoming of these studies is that they used hydrological models running at a monthly or 10-day time step, and applied a linear interpolation between model output and observed daily values of extreme discharge to estimate the climate change impact on daily based peak flow events. For a more extensive review of recent climate change related studies in the Rhine basin, the reader is referred to Vellinga et al. (2008).

No prior studies have been performed for the Rhine basin that combine and compare different downscaling methods and projections of climate change with the aim of estimating flood-peak probabilities. Methods targeted at simulating long time series of future discharges are still unexplored. Also, high quality hydrodynamic models simulating wave propagation through the main river channels and floodplains are hardly applied in climate change related hydrological modeling.

In this Chapter, we aim to improve the estimation of future low probability flood-peak events in the Rhine basin. We will use an approach that enables the use of RCM output and a weather generator for creating long, resampled time series of climate change scenarios as input for hydrological (daily) and hydrodynamic (hourly) modeling for the Rhine basin. We will apply this approach on three parallel modeling chains, where the difference lies in the transformation method (delta change approach, direct, and bias-corrected direct) of different RCM outputs to hydrological model input. The results are compared and analyzed for the control climate period (1961–1995) and the projection year 2050, both at basin-wide and sub-basin scale.

Figure 3.1: Map of the Rhine basin.

The Chapter is structured as follows. Section 3.2 shortly describes the Rhine basin. In Section 3.3 the method is introduced, specifying the hydrological, statistical and climate models. Section 3.4 evaluates changes in precipitation, and Section 3.5 evaluates simulated discharge and flood-peak probabilities. Finally, the discussion and conclusions are presented in Sections 3.6 and 3.7.

3.2 The Rhine basin

3.2.1 Geographical Characteristics

The Rhine is a cross-boundary river located in North-West Europe and has a length of ca. 1320 km. It originates in the Swiss Alps, and flows through parts of Germany, France, and Luxembourg, before it enters the Netherlands at Lobith (Figure 3.1). The Rhine basin comprises an area of ca. 185 000 km^2, of which the major part (160 800 km^2) lies upstream of Lobith. About 51% of the Rhine basin is used for agriculture, 39% is forested, 5% is built-up area, and the remaining 5% is surface water or bare rock and glaciers (Disse and Engel, 2001; Middelkoop et al., 2001).

Table 3.1: Basin and sub-basin discharge characteristics. Surface area (km^2) is defined by the basin area upstream of the gauging station.

Basin	Gauge	Surface area (km^2)	Mean Q (m^3/s)	Min Q (m^3/s)	Max Q (m^3/s)	Mean annual max Q (m^3/s)	Data period
Rhine	Lobith	160 800	2302	665	11 885	6781	1961–2004
Rhine	Andernach	139 549	2116	618	10 406	6494	1961–2004
Mosel	Cochem	27 088	334	10	4020	2190	1961–2004
Lahn	Kalkofen	5304	48	0	730	364	1961–2004
Main	Raunheim	27 142	176	44	1991	1043	1989–2005
Neckar	Rockenau	12 710	141	3	2105	1133	1971–1990
Rhine	Maxau	50 624	1297	379	4430	3191	1961–2004

The Rhine basin is densely populated and the river is intensively used for inland shipping (Jonkeren et al., 2007). The Rhine also provides water supply for the cooling of energy plants, and for industrial, domestic, and agricultural purposes (Grabs, 1997). In order to protect vital economic activities in the Rhine basin, dikes have been constructed in the lower Rhine delta since the 19^{th} century and they have been widened and heightened since. To facilitate inland shipping, the main Rhine branch has been straightened and weirs have been constructed. As a result, the river Rhine is currently a completely regulated river system (Lammersen et al., 2002). Two extreme peak discharge events that caused flooding in the Lower Rhine and near flooding the Netherlands in 1993 and 1995 exemplified the vulnerability of the river basin to extreme flood peaks.

3.2.2 Hydrological Characteristics

A substantial amount of precipitation in the Alpine area is stored temporarily as snow in winter (DJF). Both rainfall and meltwater contribute to discharge generation, depending on the season (Pinter et al., 2006). Table 3.1 describes the basin and sub-basin characteristics. The mean annual discharge at the Lobith gauging station is ca. $2300\,m^3/s$, and the maximum observed discharge is $12\,600\,m^3/s$ in 1926. Extreme flood events mainly occur during the winter period. During such events, meteorologic low-pressure systems cross the basin while releasing great amounts of rainfall that can last for several days. Research on flood genesis of historical floods in the Rhine basin shows that frozen soils can lead to more extreme runoff volumes, when they prevent rainfall to infiltrate (Engel, 1997). Sudden melting of snow and frozen soils can also contribute to extreme floods (Disse and Engel, 2001). As a result of the size and shape of the basin, both the volume and height of the discharge peak strongly depend on the direction, speed, and rainfall intensity associated with the low-pressure systems, and depend less on the intensities of individual storms. Therefore, different

flood events show quite different geneses. The variability of the 10-day precipitation volume over the whole basin, however, seems to correlate well with the variability in peak discharge in winter (DJF) at the Lobith gauging station (Beersma et al., 2008).

Changes in the future discharge regime are therefore determined by (Beersma et al., 2008):

1. The variation and change in the amount of precipitation and evaporation during the different seasons. The change in evaporation affects mainly low and summer flows.
2. Change in temperature that will change the distribution between snow (delayed runoff) and rainfall (direct runoff) in the Alpine region, particularly in winter. Temperature thus determines the length of the snow season and affects the regime of the river.
3. The change in the (relative) variability of multi-day precipitation amounts for the Rhine, and especially the 10-day precipitation amounts. This affects in particular the magnitude of peak flows at Lobith. Increases of the 10-day precipitation variability tend to increase peak flows while decreased variability leads to decreased peak flows.
4. The timing of peak flows entering the main branch from the major sub-basins determines the magnitude of the flood peak further downstream. Changes in flood management strategies, together with meteorological changes, can affect this timing.

Most floodplains are embanked, which narrows the riverbed leading to increased peak water levels. The safety levels of embankments vary between the different riparian countries of the Rhine basin. In Germany, safety levels vary between 1/200 to 1/500 per year, while in the Netherlands the once in 1250-year flood (now estimated at $16\,000\,\mathrm{m^3/s}$ at Lobith) is the boundary condition for designing dike heights (Lammersen et al., 2002; Diermanse, 2004). Because safety levels in the Rhine basin are relatively high, the design discharges estimated by using extreme value distributions are uncertain since observed discharge records only exist for 110 years (Klemeš, 2000a,b; Sprokkereef, 2001). In practical handbooks, it is recommended that at least 200 years of discharge data are needed to confidently estimate the once in 100 year event (e.g. Shaw, 2002).

3.3 Methodology

The research approach followed in this Chapter (see Figure 3.2) compares three different methods; each one using weather generators to obtain long time series of

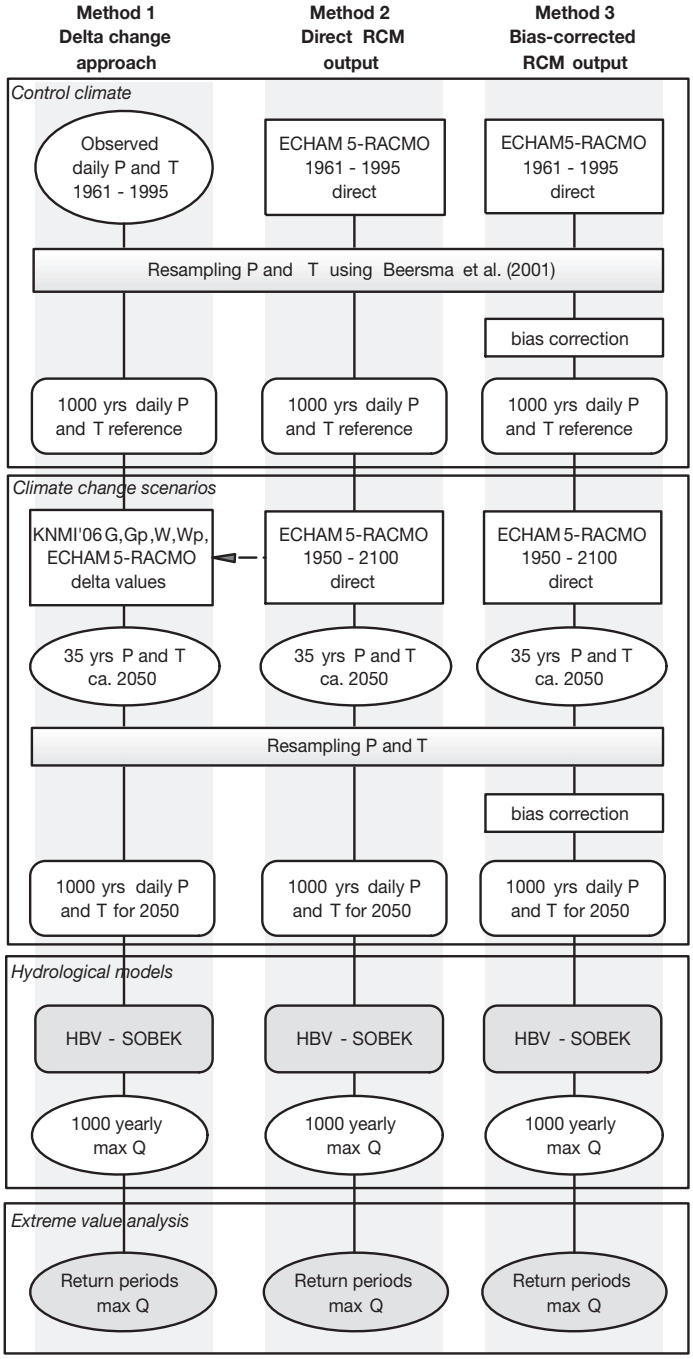

Figure 3.2: Flowchart displaying all modeling steps.

Table 3.2: Delta values of climate change scenarios for the year 2050, based on decade values and displayed per season, compared to basin-wide, seasonal means of observed temperature and precipitation. RACMO refers to the RCM simulation ECHAM5-RACMO2.1, and G, Gp, W and Wp are four KNMI'06 scenarios, based on a suite of GCM and RCM simulations. The four KNMI'06 scenarios are separated based on expected temperature rise in 2050 (moderate (G) and warm (W)), and on scenarios with (p) or without (-) a strong change in atmospheric circulation.

Temperature (°C)	DJF	MAM	JJA	SON	Year
Observed 1961–1995	0.18	7.38	15.92	8.4	7.97
dT G (°C)	0.89	0.88	0.86	0.87	0.87
dT Gp (°C)	1.15	1.27	1.40	1.28	1.27
dT W (°C)	1.78	1.75	1.71	1.74	1.75
dT Wp (°C)	2.30	2.54	2.80	2.56	2.55
dT RACMO (°C)	1.52	1.36	1.66	1.50	1.51

Precipitation (mm/day)	DJF	MAM	JJA	SON	Year
Observed 1961–1995	2.60	2.61	3.21	2.59	2.73
dP G (%)	3.62	3.02	2.77	2.94	3.09
dP Gp (%)	7.09	3.05	−9.54	−3.00	−0.60
dP W (%)	7.24	6.05	5.54	5.89	6.18
dP Wp (%)	14.18	6.11	−19.07	−6.00	−1.20
dP RACMO (%)	5.38	−0.42	−4.72	1.58	0.45

daily discharge under different climate change scenarios for 2050 (Dettinger, 2005; Orlowsky et al., 2007). All methods use the same nearest neighbor resampling technique to extend the relatively short time series ($\sim$35 years) to 10 000 years (Beersma et al., 2001; Buishand and Brandsma, 2001; Leander and Buishand, 2007). Bakker and Van den Hurk (2009) showed that the statistical properties of the resampled time series are close to the statistical properties of the input data. We applied this resampling technique within three methods that either use historical time series or RCM outputs as baseline climate information (Figure 3.2).

The first method uses historical climate data (1961–1995) (Sprokkereef, 2001) that are converted to a climate change scenario using the delta change approach. The second method directly uses the output from an RCM simulation (ECHAM5-RACMO2.1: 1950–2100). The third method uses the same RCM output but applies an additional bias correction. The three methods result in three time series of 10 000 years of precipitation and temperature. Periods of 1000 years of daily values were then used as input to a hydrological and a hydrodynamic model in order to calculate 1000 years of annual maximum discharges and their probabilities (estimated by extreme value analysis). All methods and modeling steps are shown in Figure 3.2 and are further described in detail in the following sections.

3.3.1 Generating long meteorological time series for different climate change scenarios in 2050

Method 1: delta change approach

In 2006, the Royal Netherlands Meteorological Institute (KNMI) presented four new climate scenarios for the Netherlands (Van den Hurk et al., 2006, 2007). The KNMI'06 climate scenarios are based on a suite of GCM and RCM simulations produced within the European PRUDENCE project (Christensen et al., 2007; Lenderink et al., 2007b). In PRUDENCE, dynamical downscaling was applied using 10 RCMs and 5 GCMs, all for two 30-years time slices: a control period 1960–1990, and a future period 2070–2100. The projected changes for 2050 result from linear interpolation between these dates. The simulation results show variable changes in projected strength of westerly winds in the Rhine basin area. A strong change in atmospheric circulation is expected to result in milder and wetter winters due to more westerly winds (Gp and Wp), when compared to scenarios without atmospheric circulation change (G and W). Hence, both temperature and changes in the atmospheric circulation are used as steering parameters to discriminate four climate change scenarios. The KNMI'06 scenarios are summarized in Table 3.2; they all describe a plausible range of possible future climate conditions, based on best available knowledge, and no statement is made on the probability of occurrence of a given scenario. Because of large uncertainties at a spatial scale smaller than the Netherlands, the KNMI provided uniform scenarios for the Netherlands, which we uniformly applied for the whole Rhine basin.

A historical data set from the International Commission for the Hydrology of the Rhine basin (CHR) was used to describe the control climate for the 134 sub-basins that are used in the HBV model (see Section 3.3.2). This data set contains daily values of precipitation and temperature for the years 1961 to 1995, which are based on 174 measurement stations throughout the basin (Sprokkereef, 2001).

Decadal values of the KNMI'06 climate scenarios were used to perturb the resampled historical data set of daily precipitation and temperature for the period 1961–1995 (i.e. the delta change approach (Lenderink et al., 2007a; Te Linde, 2007)). For this purpose, a year was divided in 36 decades of days (3 decades per month). The first two decades of a month always consist of 10 days and the third decade covers the remaining days.

For comparison reasons, we also applied this approach using delta values of the ECHAM5-RACMO2.1 scenario (see Method 2). Decadal basin averages were calculated for the control period (1961–1995) and the future period (2036–2065). Subsequently, these decadal values were smoothed using a moving average with a window of seven decades. The decadal delta values were obtained from these smoothed decadal

averages. The basin-wide seasonal delta values of RACMO precipitation and temperature are summarized in Table 3.2, where the KNMI'06 scenarios are also displayed.

This simple delta approach is widely used in water management practices (e.g. Aerts and Droogers, 2004; Andréasson et al., 2004) but the delta change approach has limitations. First, as the KNMI'06 represent spatially uniform scenarios, applying these will not take into account possible geographical differences in the change of precipitation and temperature. Second, the present day variance of temperature and the coefficient of variation of precipitation are left unchanged, while changes in variance due to climate change are expected. Third, possible changes in the number of precipitation days are not considered.

We evaluated the effect of the ECHAM5-RACMO2.1 scenarios and all four KNMI'06 scenarios on monthly mean discharge (G, Gp, W and Wp). To reduce the number of simulations, we only compared one KNMI'06 scenario (Wp) to ECHAM5-RACMO2.1 on yearly maximum discharges and flood-peak probabilities. Wp was chosen because it is the most extreme of the four scenarios.

Method 2: direct output ECHAM5-RACMO2.1

To overcome the limitations of the delta change approach, we applied a second method that uses direct output from a regional climate model RACMO2.1 for the years 2036–2065 (hereafter referred to as RACMO) (Lenderink et al., 2003; Meijgaard et al., 2008). This RCM is forced by the ECHAM5-GCM member 3 output forced by the SRES-A1B emission scenario. RACMO output consists of daily data at a spatial resolution of 25×25 km. Its results suggest a transformation of the dry and wet frequency, variance and spatial variability for a future climate in 2050. Earlier versions of RACMO performed well in simulating precipitation climatology in the Rhine area (Van den Hurk et al., 2005) and mean and interannual variability of summertime temperature (Lenderink et al., 2006). We used Thiessen polygons to transform the grid-based output of RACMO to 134 sub-basins that are necessary to run the HBV model of the Rhine (see Section 3.3.2).

Method 3: Bias-corrected output ECHAM5-RACMO2.1

Finally, a third method was used that improves the direct RCM output by applying a bias correction (Wilby et al., 2000; Wood et al., 2004; Orlowsky et al., 2007). Bakker and Van den Hurk (2009) compared the ECHAM5-RACMO2.1 output to observed values for the control climate period (1961–1995) and several biases were identified. A bias correction method was developed that considerably improves the spatial and monthly variability and statistics of extreme values of large-scale multi-day rainfall. The monthly bias was determined for all 134 subcatchments separately. RACMO

substantially overestimates the number of wet days (daily precipitation $> 0.05\,\mathrm{mm}$). A correction was applied that reduces the change of the probability distribution of precipitation amounts on wet days to a minimum (bias correction 1). Based on the distribution function, target amounts for the required removal of wet days are set. Next, days with values close to this target amounts are selected and given zero precipitation. Days are only selected for drying if four of the six surrounding days are dry as well. This selection criterion leaves the multiday variability and extremes in tact. After adjusting the number of wet days, the mean (bias correction 2) and coefficient of variation (bias correction 3) are corrected by applying a power-law function. The monthly coefficients of the power-law function are calculated for the 134 subcatchments separately.

3.3.2 Hydrological models

Simulation of rainfall-runoff

We used the semi-distributed conceptual HBV model (Hydrologiska Byråns Vattenbalansavdelning) (Bergström, 1976; Lindström et al., 1997) to simulate discharge on a daily basis. HBV is a soil moisture accounting model. It uses daily values of precipitation and temperature, and monthly potential evapotranspiration as input. The model uses different routines in which snowmelt is computed by a degree-day relation, and groundwater recharge and actual evaporation are functions of the water storage in a soil box. Discharge formation is presented by three linear reservoir equations and the sub-basins are linked with a simplified Muskingum approach to simulate the routing processes (see Appendix A). The HBV model for the Rhine is applied to 134 sub-basins and was developed in 1999 (Eberle et al., 2005). Potential evaporation is transformed by temperature at a daily basis, and is based on monthly potential evapotranspiration values. Potential evapotranspiration values differ between land use classes and are based on several studies by the German Bundesanstalt für Gewässerkunde (Eberle et al., 2005). When implementing a climate change scenario in HBV, monthly potential evapotranspiration values remain the same, but actual evaporation values are influenced by changes in temperature. The daily-based HBV model we used in the current study performs well for the Rhine (Nash&Sutcliffe=0.85, r^2=0.97, for 1993), as is further described in Eberle et al. (2005) and Te Linde et al. (2008a).

Simulation of flood wave propagation in the main river

The routing scheme in HBV is not capable of simulating flood wave propagation, backwater effects, and damping in low gradient river stretches where floodplain in-

undation plays an important role. Therefore, a 1D-hydrodynamic model (SOBEK) was used to simulate flood routing in the main Rhine branch at an hourly time step (Delft Hydraulics, 2005) (see Appendix B). SOBEK is an integrated numerical modeling package and is based on the 1D Saint Venant equations (Chow, 1959). This model allows the implementation of structural measures, such as dike heightening, dike relocation, weirs, and detention areas. Cross sections at every 500 m, and dike locations, dike heights, and detention areas as they currently exist in the Rhine are schematized in the model. The assumption was made, though, that under current circumstances no flooding occurs in the Rhine basin. To reduce computing time, SOBEK was only used to simulate discharge during a 30-day window around the yearly maximum peak discharge, and in those calculations HBV output for the subbasins were used as boundary conditions. The increased performance on estimating peak flows due to SOBEK is described in Eberle et al. (2004). Extreme flood peaks ($>8000\,\mathrm{m}^3/\mathrm{s}$ at Lobith) were overestimated by an average of 5% when only HBV was used, which reduced to an average of 2% when the routing scheme in HBV was replaced by SOBEK, but the results showed large variations (up to 20% overestimation by HBV).

3.3.3 Extreme value analysis

The current practice in river management in the Netherlands to estimate the Q_{1250} design discharge, is to fit the Gumbel, the log-normal and the Pearson-III distributions on the annual maximum discharges at the Lobith gauging station (Diermanse, 2004). The Gumbel fit is mostly used in visualizations of extreme value analysis at Lobith. We chose to extend the Gumbel or type I extreme value distribution by adding a shape parameter so it evolves into the Generalized Extreme Value distribution (GEV) (see Appendix C). Three types of extreme value distribution functions ($F(x)$) are combined into the GEV distribution:

$$F(x) = \exp\left\{-\left(1+\beta\frac{x-\gamma}{\delta}\right)^{\frac{1}{\beta}}\right\}$$

where γ is the location parameter, δ is the scale parameter, and β is the shape parameter. When $\beta = 0$, the GEV corresponds to the type I (Gumbel) distribution; $\beta < 0$ corresponds to the type II (Fréchet) distribution; and $\beta > 0$ corresponds to the type III (Weibull) distribution, which has a finite upper limit. We plotted the GEV distribution on Gumbel paper, creating a concave curve instead of a straight line when $\beta \neq 0$. The maximum likelihood approach was used to estimate the distribution parameters. The exceedance probability denotes the probability that a certain discharge value will be exceeded in one year. In this Chapter, we mainly use the

Table 3.3: Basin-wide, seasonal means of observed temperature and precipitation, compared to simulated historical temperature by RACMO (control climate experiment, 1961–1995).

Temperature (°C) 1961–1995	DJF	MAM	JJA	SON	Year
Observed	0.18	7.38	15.92	8.40	7.97
RACMO (method 2)	2.02	8.19	16.00	9.30	8.90
RACMO (method 3)	0.60	7.95	16.49	8.81	8.50

Precipitation (mm/day) 1961–1995	DJF	MAM	JJA	SON	Year
Observed	2.60	2.61	3.21	2.59	2.73
RACMO (method 2)	3.32	3.11	2.92	3.07	3.10
RACMO (method 3)	2.87	2.65	3.03	2.72	2.80

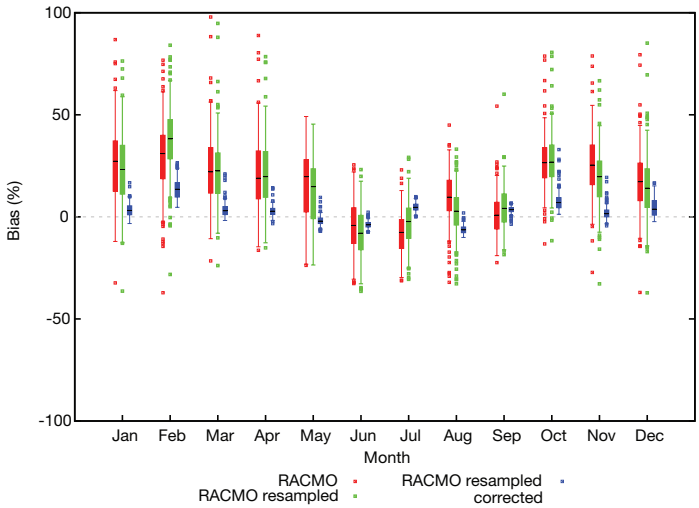

Figure 3.3: Box-whisker plots of monthly biases of the 134 sub-basins in mean precipitation. The black line denotes the median, the solid box denotes the range from 25^{th} to 75^{th} percentiles of the sample, and the whiskers show the data range. The outliers (dots) are defined as values that are more than 1.5 times the interquartile range away from the top or bottom of the box.

term return period, which denotes the mean interval between two events of the same intensity and is the inverse of the exceedance probability.

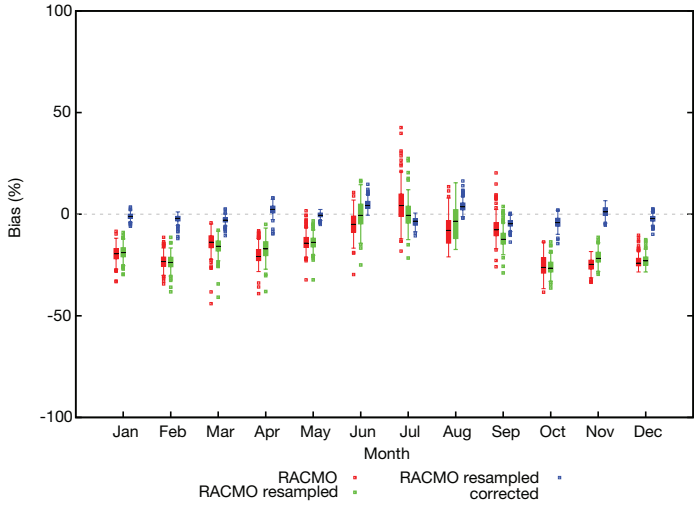

Figure 3.4: Box-whisker plots of monthly biases of the 134 sub-basins in the coefficient of variation (CV) of the precipitation.

3.4 Evaluation of changes in precipitation and temperature

3.4.1 Comparing observed and RACMO data for the control climate (1961–1995)

Here we show the quality of the RACMO regional climate model in reproducing the observed precipitation and temperature, where we compare method 2 (no bias correction) and 3 (with bias correction). Figure 3.3 and 3.4 show the distribution of the monthly biases of the 134 sub-basins for the mean precipitation and for the coefficient of variation (CV), respectively. In the winter months, the mean precipitation is substantially overestimated, up to biases of almost a factor two in some sub-basins in Switzerland. Conversely, the winter CV is substantially underestimated. RACMO (method 3) resembles summer characteristics of both the mean and the CV of observed precipitation much better. However, there is a large spatial spread in biases in both the mean and the CV over the Rhine basin for all months. Seasonal changes in basin-wide means of precipitation and temperature obtained by RACMO (method 2 and 3) are compared to observed values in Table 3.3. It displays that the seasonal basin-wide precipitation and temperature means are represented well by RACMO after bias correction (method 3).

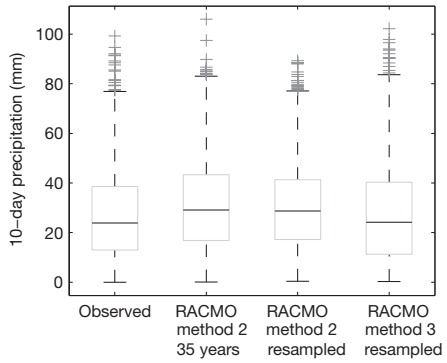

Figure 3.5: Box-whisker plots of basin-wide average 10-day precipitation for the control climate (1961–1995)

The box-whisker plots of basin-wide average of 10-day precipitation for the control climate in Figure 3.5 show that the median is overestimated by RACMO (method 2) by 20%, and that the 1st and 3rd quartiles are overestimated by 7–30%. Figure 3.5 also shows that the resampling of the RACMO output (method 2) hardly changes the general statistical characteristics when compared to the 35 years of RACMO output for the control climate period. This demonstrates that errors due the use of the stochastic rainfall generator can be considered small compared to the errors resulting from GCM–RCM simulations. This was expected since the resampling is designed to preserve the general statistical descriptors while generating very long time series including extreme multiday precipitation events. In addition, Figure 3.5 shows that after the bias correction the resampled RACMO output resembles observed values very well. The median is now overestimated by 1% only. Bakker and Van den Hurk (2009) further explains that the yearly pattern in the bias in both the median (Figure 3.3) and the CV (Figure 3.4) largely disappeared and that the spatial distribution of the bias considerably decreased after bias correction.

To evaluate the performance for extreme peak rainfall events, the yearly maxima of 10-day values are plotted against their return period in Figure 3.6. The figure shows the extreme value distribution of observed values of 1961–1995, 2500 years resampled observed values, 2500 years resampled RACMO output for the control climate (method 2), and 10 000 years of bias corrected RACMO output (method 3) for both the control climate and the future climate (2050). Increasing the number of data points from 35 to 2500 or 10 000 results in smoothing of the extreme value distributions. Contrary to the median and the 1st and 3rd quartiles (Figure 3.5), the Rhine basin average 10-day precipitation amounts obtained by method 2 are largely underestimated when compared to (resampled) observed values. The 10-day precipitation extremes poorly resemble the 10-day extremes as assessed by resampling

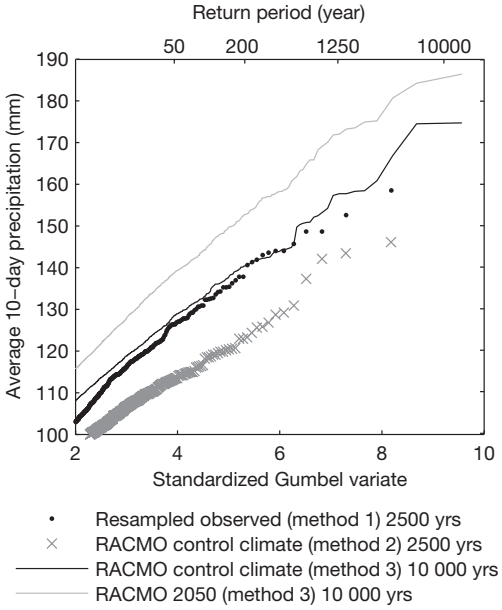

Figure 3.6: Extreme value plot of basin wide, resampled 10-day precipitation values. Displayed are 2500 years of resampled observations of the control climate (1961–1995, black dots), 2500 years of RACMO method 2 for the control climate (red crosses), 10 000 years of RACMO method 3 for the control climate (green line), and 10 000 years of RACMO method 3 for 2050 (blue line).

of the observed time series (method 1). After correction, the large extremes with return periods of 10 years and more fit the extremes of resampled observed time series very well (Figure 3.6). The large improvement of the RACMO output after bias correction emphasizes the need for bias correction of RCM output. For a more complete description of the bias correction of RACMO output and a more elaborate discussion of the resulting changes in precipitation and temperature for the control climate, see Bakker and Van den Hurk (2009).

3.4.2 Climate change scenarios: comparing ECHAM5-RACMO with the delta change approach

Projected changes in mean seasonal values of temperature and precipitation for the year 2050 are displayed in Table 3.2. According to the climate change projections, a rise in mean annual temperature of 0.9°C for the G scenario and 2.6°C for the Wp scenario can be expected by 2050. With a value of 1.5°C, the bias-corrected RACMO scenario lies just below the middle of those scenarios. Changes in projected precipitation vary considerably between scenarios and seasons. The G and W scenarios project an increase of precipitation by 3 and 6% in all seasons, while the Gp scenario is comparable to the W scenario in the winter, but shows a decrease in mean precipitation by 9.6% in the summer. The Wp scenario projects the most extreme increase of 14.2% during the winter months and a decrease in precipitation in summer and early autumn up to 19.1%. Like the projections for changes in temperature, the RACMO precipitation scenario falls in between all four KNMI'06 scenarios. It displays an increase of 5.4% in mean precipitation in the winter months and a decrease of 4.7% in the summer months. Van den Hurk et al. (2006) compared mean seasonal change in precipitation and temperature of the GCMs that are used to construct the KNMI'06 scenarios. This study showed that the ECHAM5 output used to force RACMO was positioned near the average values of those GCMs, which explains the observations above.

3.5 Evaluation of simulated discharge and flood-peak probabilities

The impact of climate change on the simulated change in discharge behavior is analyzed both on mean monthly discharge values and on daily flood peaks. In the following paragraphs, first the effects of methods 2 and 3 (RACMO runs with and without bias correction) on present-day simulated flood-peak probabilities are compared. Second, the performance of simulated discharge by method 3 at sub-basin scale is analyzed by comparing basic statistical descriptors for the control climate period

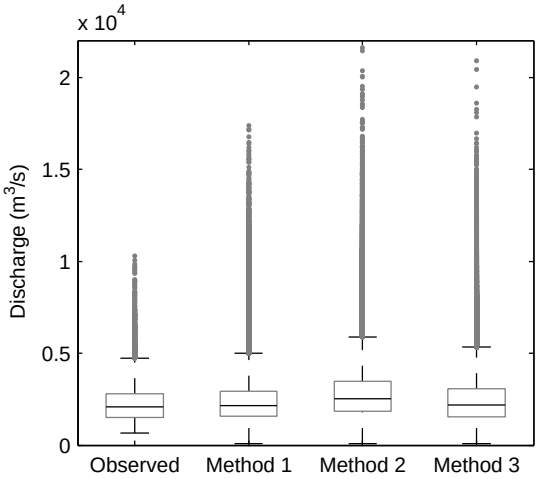

Figure 3.7: Box-whisker plots of daily values of observed and simulated discharges for the control climate (1961–1995) at Lobith. Displayed are observed discharges (35 years) and simulation results from different resampled forcing datasets (1000 years): observed precipitation and temperature (CHR, method 1),; direct RACMO output (method 2); and bias-corrected RACMO output (method 3).

with the observed discharge (1961–1995). Third, the projected impact of different climate change scenarios on mean monthly discharge is evaluated for all three methods. Finally, the impact of climate change on flood-peak probabilities is examined, again using each method.

3.5.1 Effect of meteorological bias correction on simulated discharge and flood-peak probabilities for the Control Climate (1961–1995)

Section 3.4.1 showed that the bias-corrected RACMO output well resembles both mean and extreme values of observed precipitation and temperature, in contrast to direct RACMO output. Here we discuss the effect of the bias-corrected data on simulated discharge at the Lobith gauging station. In order to evaluate which forcing data result in a good representation of current discharge behavior, we have compared discharge observations with simulated values resulting from HBV forced with observed meteorological data (method 1) and different RACMO outputs (method 2: direct, and method 3: bias-corrected, see Figure 3.2). The result of this comparison is displayed in a box-whisker plot (Figure 3.7). The many outliers of yearly maximum values in this plot show the skewed distribution of daily discharge. When compared to

precipitation in Figure 3.5, the daily discharge is much more skewed than 10-day precipitation volumes. The use of method 1 slightly overestimates the median (4%) and other quartiles of discharge when compared to observed discharges. The many more outliers are a direct result of the sampling size (35 years vs. 1000 years). When RACMO output is directly used as forcing data (method 2), the median of simulated daily discharge is overestimated by $470\,m^3/s$ (23%). All simulated discharges appear to be higher than observed and the interquartile range is wider than for observed values. Also, direct RACMO output (method 2) results in more extreme flood peaks (outliers) than method 1 for the control climate. The bias-corrected precipitation and temperature generated by RACMO (method 3), though, result in a simulated median discharge of $2177\,m^3/s$, which is an over estimation of only 5%. Comparable small over estimations are observed for the 25^{th} and 75^{th} percentiles. Also the tail of the discharge distribution resulting from bias-corrected RACMO output resembles discharges obtained from the measured climate series (method 1) more closely than results forced by direct output. Considering basic statistical descriptors, such as medians and percentiles, bias correction of RACMO forcing data results in simulated discharge that is more similar to observed discharge than in a model structure without bias-correction.

Figure 3.10a shows yearly maximum observed and simulated discharge data (method 1) plotted against their return periods for the control climate period. A Gumbel distribution was fitted through the 100 years of observed yearly maxima at Lobith, and through the 1000 years of simulated yearly maximum discharges for the control climate period (Method 1, Figure 3.10a). Note that only yearly maxima above a threshold of $8000\,m^3/s$ are displayed in Figure 3.10, but that all values were included when fitting the extreme value distributions. Also shown are the 95% confidence intervals that can be interpreted as the statistical uncertainty of the distribution fits. At a return period of 100 years, the estimated peak discharge is $13\,000 \pm 1750\,m^3/s$ (13%) according to the width of the 95% confidence interval for observed values. The Gumbel fit through the 1000-year control climate period agrees very well with the observed data fit. The estimated peak discharge is also $13\,000\,m^3/s$ at a return period of 100 years, but the 95% confidence interval is much narrower with $\pm 450\,m^3/s$ (3%). Thus, the confidence interval narrows to a quarter of its original size while increasing the sample size from 100 to 1000 years, reducing the statistical uncertainty that results from fitting extreme value distributions and extrapolation of those fits.

The ten most extreme discharges of the 1000-year control climate period (method 1) lie around the lower 95% confidence interval, and the two most extreme peaks even lie outside the confidence intervals of the Gumbel fit. The Gumbel distribution seems a good fit for historical data, but apparently fails to describe the upper tail of the distribution of discharges according to the simulated discharge for the control climate, as is plotted in Figure 3.10a. Therefore, a shape parameter was introduced in the GEV distribution. The result for the control climate situation is shown as

the dashed line in Figure 3.10b, where it can be seen that the GEV fit bends down also describing the most extreme values of the sample. Figure 3.10b also displays the extreme discharges resulting from method 2 at Lobith for the control climate period. Contrary to our observation for extreme 10-day precipitation values in Section 3.4.1, yearly maximum discharges resulting from direct RACMO output (method 2) are overestimated when compared to observations. The overestimation varies between 8 and 25%, in the range of return periods of 50 to 1250 years, of which the latter corresponds with an overestimation of 4000 m^3/s. After bias correction (method 3) the yearly maximum discharges resemble the control climate (method 1) much better, but above 12 000 m^3/s (T=100 years) both data sets diverge and discharges resulting from RACMO (method 3) are still overestimated according to the simulation results. The difference increases up to 3500 m^3/s at a return period of 1250 years (See also Table 3.7).

As explained in Section 3.2.2, the common assumption and observation is that yearly maximum values of 10-day precipitation and discharge are closely related. Our results on the effect of bias correction contradict this; the yearly maximum 10-day precipitation was underestimated before bias correction (Figure 3.6), whereas the yearly maximum discharge was overestimated. It appears that the yearly maximum 10-day precipitation can occur in all seasons, while the yearly maximum discharge mainly occurs in winter, which might explain our observation. The overestimation of yearly maximum discharges before bias correction is in line with the overestimation of daily values of both precipitation and discharge as displayed in Figure 3.5 and Figure 3.7, respectively.

Overall, we have shown that an error in the meteorological forcing data propagates to an error in simulated peak discharges, leading to an incorrect representation when compared to observed values. The considerable improvement of simulated discharge as a result of bias correction stresses the need for bias correction of meteorological data from RCM output when using simulated discharges based on those data in climate change scenario studies.

3.5.2 Performance of simulated discharge by method 3 at sub-basin scale

One of the major differences between methods 2 and 3 on the one hand, and method 1 on the other hand, is a spatially explicit climate scenario at the RCM grid scale of 25×25 km in method 2 and 3, instead of a geographically uniform application of relative changes in precipitation and temperature as method 1 does. We therefore tested the performance of the simulated discharge obtained by method 3 at the sub-basin scale for the control climate (1961–1995). Since the resampled data set is a synthetic time series, a day-to-day comparison to observations with performance indicators

Table 3.4: Basin and sub-basin discharge characteristics for the control climate (1961–1995). Displayed are observed values and discharges obtained by method 1 (CHR 35 years and CHR resampled (1000 years)) and method 3 (bias-corrected RACMO resampled). *SD* is the standard deviation from the mean.

Basin Gauge		10^{th} percentile (m^3/s)	Mean (m^3/s)	90^{th} percentile (m^3/s)	Mean ann. max. Q (m^3/s)	*SD* (m^3/s)	Skewness –
Rhine	Observed	1156	2299	3767	6691	1204	1.96
Lobith	CHR 35 (mtd 1)	1137	2355	3921	7053	1290	1.99
	CHR (mtd 1)	1202	2456	4275	7405	1317	2.10
	RACMO (mtd 3)	1177	2525	3997	7630	1415	1.93
Mosel	Observed	81	335	736	2147	365	3.10
Cochem	CHR 35 (mtd 1)	82	340	741	2077	369	3.15
	CHR (mtd 1)	91	352	855	2134	372	3.08
	RACMO (mtd 3)	84	371	765	2217	401	2.84
Lahn	Observed	13	49	104	369	59	3.58
Kalkofen	CHR 35 (mtd 1)	6	46	111	337	59	3.31
	CHR (mtd 1)	7	50	118	374	64	3.35
	RACMO (mtd 3)	7	48	121	349	62	3.24
Main	Observed	70	164	322	995	176	4.61
Raunheim	CHR 35 (mtd 1)	66	197	409	1019	191	3.29
	CHR (mtd 1)	69	209	447	1088	207	3.46
	RACMO (mtd 3)	67	212	436	1151	221	3.45
Neckar	Observed	46	140	259	1008	141	4.38
Rockenau	CHR 35 (mtd 1)	41	141	264	936	136	4.25
	CHR (mtd 1)	43	148	304	1028	149	4.36
	RACMO (mtd 3)	37	153	278	1149	170	4.50
Rhine	Observed	691	1297	2034	3207	549	1.10
Maxau	CHR 35 (mtd 1)	667	1272	2054	3505	590	1.45
	CHR (mtd 1)	699	1334	2280	3639	610	1.50
	RACMO (mtd 3)	685	1385	2127	3964	686	1.55

that are common practice in hydrologic modeling (i.e. Nash & Sutcliffe, volume error or correlation) is not possible. We therefore compared statistical descriptors of the obtained data sets to test the performance of simulated discharge by method 3 at the basin and sub-basin scales. Table 3.4 displays the basic statistical descriptors of daily discharges for the control climate (1961–1995). We compared 35 years of observed discharge with simulated discharge by HBV that was forced with observed precipitation and temperature data (CHR data). We also used resampled CHR data (method 1) and resampled bias-corrected RACMO data (method 3) to create 1000 years of simulated discharge and compared those to the other data sets. In this way, we distinguished:

1. the difference between observed and simulated discharge by HBV resulting from observed meteorological data (CHR 35),

Table 3.5: Seasonal change in discharge at Lobith according to KNMI'06 scenarios and bias-corrected RACMO output, for 2050.

Discharge (m^3/s)	DJF	MAM	JJA	SON	Year
Control climate (1961–1995)	2778	2518	2314	1809	2355
dQ G (mtd 1) (%)	6.71	2.03	−2.16	1.47	2.01
dQ Gp (mtd 1) (%)	5.58	3.00	−17.40	−17.63	−6.61
dQ W (mtd 1) (%)	13.04	4.47	−3.94	3.02	4.15
dQ Wp (mtd 1) (%)	10.56	6.50	−31.68	−33.25	−11.97
dQ RACMO (mtd 3) (%)	14.20	−0.75	−17.36	−12.63	−4.14

2. the difference between simulated discharge resulting from observed and from resampled observed meteorological data (CHR resampled, method 1),

3. the difference between simulated discharge resulting from resampled observed meteorological data (CHR resampled, method 1) and from resampled RACMO output (method 3).

The distribution of the discharge at Lobith and from the Upper Rhine is less skewed than from the other sub-basins, as shown in Table 3.4. This can be explained by the snowmelt component in the discharge regime of the Alpine area in the Upper Rhine. Snowmelt results in higher base flow values and therefore displays a less skewed probability distribution than discharge from mainly rain fed sub-basins. For the 10^{th} percentile, the mean, the 90^{th} percentile, and the skewness, all three simulated discharge data sets agree very well with observed values for all sub-basins. The standard deviation of discharge data obtained by method 3, though, is somewhat higher for all basins, except for the Lahn. Together with the observation that the mean annual maximum is overestimated by method 3 for the same basins, it follows that this data set contains slightly higher peak discharges than observed. Overall, the simulated discharge obtained by method 3 resembles the observed spatial structure in the discharge regime very well.

3.5.3 Climate change impact on monthly mean discharge

Mean seasonal and monthly changes in discharge for Lobith were analyzed in detail, and for several sub-basins for the winter season only. The impact of different climate change scenarios on discharge is displayed for Lobith in Table 3.5 (seasonal) and Figure 3.8 (monthly). When applying the KNMI'06 scenarios (method 1, Figure 3.2), mean winter discharge is expected to increase between 6.7% (G) and 13.0% (W). However, the projected decrease in summer and autumn stands out, ranging between −2.2% (G) and −33.3% (Wp), and this range is even more emphasized in monthly values (Figure 3.8) where September shows a maximum decrease of −40%. The bias-

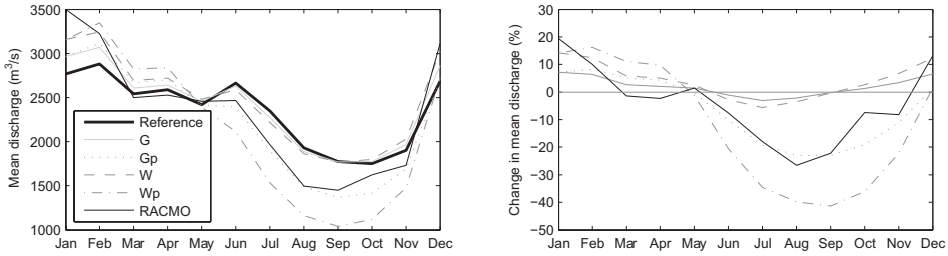

Figure 3.8: Monthly mean change in discharge at Lobith according to KNMI'06 scenarios and bias-corrected RACMO output, for 2050, absolute values (left) and relative values (right).

corrected RACMO scenario (method 3) most resembles Gp, except for the months of January and February. In the winter months the results of RACMO (method 3) are 14.2% higher than the average observed values; this is more than can be observed in any of the four KNMI'06 scenarios. Moreover, when comparing Table 3.5 with Table 3.2, where the delta values of the seasonal change in precipitation and temperature are displayed, Wp has higher values of increase in precipitation than bias-corrected RACMO (method 3) in the winter season (14.2 vs. 5.4%). There is a non-linear relationship between the relative increase in precipitation and temperature on one hand, and resulting discharge in the winter months on the other, which is due to inherent complex hydrological and groundwater processes (Uhlenbrook, 2003; Bogaard et al., 2005). Further comparison of Table 3.2 and Table 3.5 for other seasons reveals, for example, that the relative decrease in discharge in summer and autumn is higher than the relative decrease in precipitation volume. It is likely that the projected temperature increase results in higher evaporation rates, and therefore lower discharges. Our results on projected monthly mean change in discharge are in agreement with values obtained by previous studies on climate change in the Rhine basin (Van Deursen, 2002; Kwadijk and Rotmans, 1995; Middelkoop and Kwadijk, 2001).

Mean changes in discharge in winter months at the sub-basin scale are displayed in Figure 3.9, where only the results for the Wp (method 1) and RACMO (method 3) scenarios are shown. Both scenarios roughly display the same spatial structure, with the largest increase in discharge in the Main (19–30%), followed by the Neckar, the Lahn, and the Mosel (13–24%), and the smallest changes upstream of Maxau in the Alpine area (7–18%) and in the Middle and Lower Rhine (0–12%). Compared to the basin-wide changes (Table 3.5), these results imply that mean winter discharge increase in the Main can be almost twice the basin-wide increase. The RACMO scenario shows much more geographical differentiation in mean change in winter discharge between sub-basins than the Wp scenario, due to spatial differentiation in the RACMO output of precipitation and temperature for 2050.

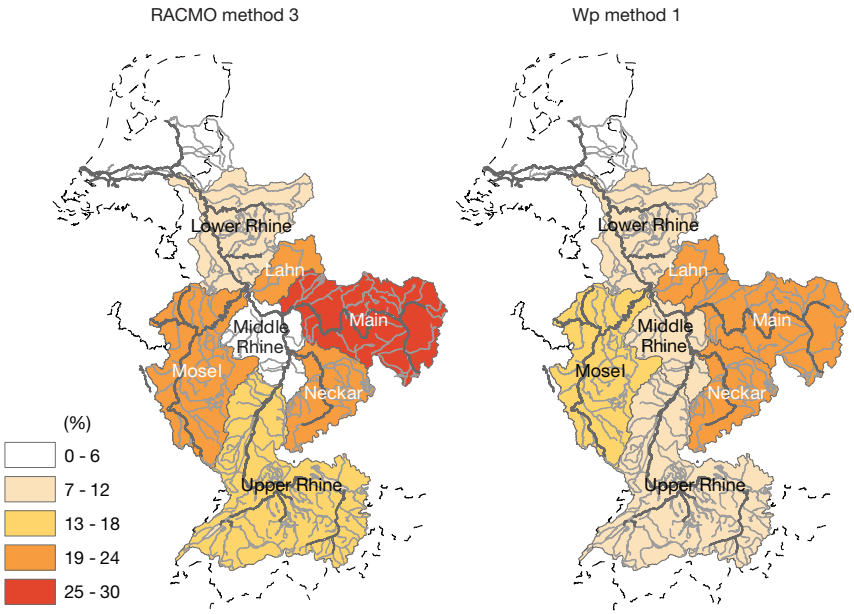

Figure 3.9: Mean change in winter discharge for the Wp and bias-corrected RACMO scenarios for 2050.

Table 3.6: Statistical parameters of yearly maximum discharges for the control climate (1961–1995) and two climate change scenarios for 2050. All four data sets contain 1000 simulated yearly maxima. SD is the standard deviation from the mean.

Lobith	Mean	SD	Skewness	Min	Max	25%	75%
					percentile	percentile	
Control clim. CHR (mtd 1)	6327	2192	0.84	2011	15 694	4702	7705
Control clim. RACMO (mtd 3)	5623	2498	1.08	863	19 801	3714	7104
2050 Wp (mtd 1)	7301	2651	0.76	1757	18 215	5347	8999
2050 RACMO (mtd 3)	6534	2941	1.07	1326	25 110	4402	8303

The relatively modest increase that we project in the Alpine area in Figure 3.9 is probably the consequence of only displaying the winter season (DJF), while Alpine increase is very likely most profound in the spring. Stewart (2008) compared different studies of observed and projected changes in snow cover and snowmelt-derived streamflow for the European Alps, and summarizes that a general decrease in annual snowpack, and earlier spring snowmelt runoff have been observed. Under a warming climate, the Alpine mountain range will lose some of its functions as seasonal water storage. A detailed study by Bavay et al. (2008) on two Alpine headwater catchments project a much narrower snowmelt discharge peak in spring, and heavy precipitation events in the fall are expected to change from mainly snow-fed to mainly rain-fed.

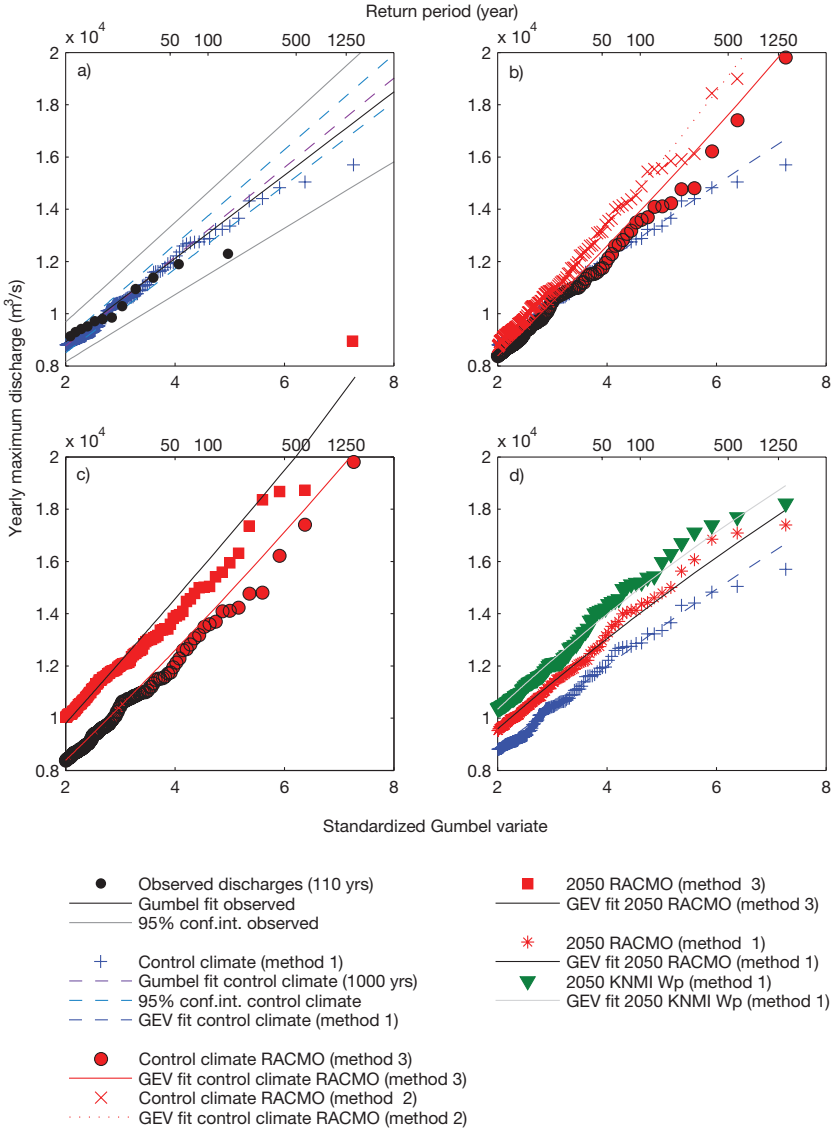

Figure 3.10: Extreme value distributions and GEV fits of yearly maximum discharge at Lobith for the reference situation and the year 2050. Displayed are (a) 100 years of observed data and 1000 years of resampled and modeled data for the control climate (method 1, 1961–1995) and Gumbel distribution fits projected as a straight line with 95% confidence intervals; (b) control climate, and RACMO (method 2 and 3) for the control climate; (c) control climate, and RACMO (method 3) for 2050; (d) control climate, RACMO (method 1), and Wp (method 1) for 2050. Notice the scale difference between 10c and the others. Note that only yearly maxima above a threshold of 8000 m^3/s are displayed, but that all values were included when fitting the extreme value distributions.

Table 3.7: Discharge in m^3/s at Lobith at different return periods (T) for the control climate (1961–1995) and under climate change. The numbers based on their GEV fits, displayed in Figure 3.10.

		T (yr)					
	Scenario	10	50	100	200	500	1250
Control clim.	CHR (mtd 1)	9 234	11 802	12 821	13 801	15 038	16 216
Control clim.	RACMO (mtd 3)	8 896	12 392	13 933	15 508	17 647	19 856
2050	Wp (mtd 1)	10 824	13 809	14 970	16 070	17 442	18 726
2050	RACMO (mtd 3)	10 041	14 350	16 050	17 763	20 052	22 372
2050	RACMO (mtd 1)	10 056	12 844	13 935	14 972	16 271	17 492

Table 3.8: Relative changes in discharge at Lobith at different return periods (T) under climate change. First displayed is the relative change in %, where RACMO (method 1) and Wp (method 1) are related to CHR (method 1) for the control climate and RACMO (method 3) for 2050 is related to RACMO (method 3) for the control climate. These changes in % are then used to calculate the absolute discharges of RACMO (method 3) that are displayed in the second part ('relative').

		T (yr)					
Discharge	(%)	10	50	100	200	500	1250
2050	RACMO (mtd 1)	8.9	8.8	8.7	8.5	8.2	7.9
2050	Wp (mtd 1)	17.2	17.0	16.8	16.5	16.0	15.5
2050	RACMO (mtd 3)	16.9	15.8	15.2	14.5	13.6	12.7
Discharge	(m^3/s)						
2050	'Relative' RACMO (mtd 3)	10 796	13 666	14 769	15 807	17 088	18 271

3.5.4 Climate change impact on flood-peak probabilities

Basin-wide results at the German–Dutch Border (Lobith)

The probability and volume of extreme peak values is generally of higher interest than the projected changes in mean monthly discharge. Climate change impacts on flood peak events with return periods of 200 to 1250 years were further investigated, since these are the safety levels in the Rhine basin (see Section 3.2). Yearly maximum discharges of 1000 years for the control climate (1961–1995, method 1 and method 3, see Figure 3.2), the RACMO scenario with bias correction for 2050 (method 3) and the Wp scenario for 2050 (method 1) are depicted in Table 3.6. RACMO (method 2) is not displayed or discussed in this Section. Mean yearly maximum discharge is expected to increase by 981 m^3/s according to the Wp scenario (method 1), whereas RACMO (method 3) shows an increase of 911 m^3/s, when compared to RACMO for the control climate. RACMO (method 3) results in a higher skewness and standard deviation, indicating a wider probability distribution of the yearly maxima than values

obtained by method 1. This results from the overestimation of discharge peaks above 12 000 m^3/s at Lobith by RACMO. Both by RACMO and Wp obtained maximum values under climate change in 2050 indicate a substantial increase compared to the maximum obtained discharge in the control climate period (Table 3.6).

The probability of reaching discharges in this range is estimated by extreme value analysis. In Figure 3.10c the results of RACMO (method 3) are displayed for 2050 relative to the control climate, with GEV distributions fitted through the data. Notice the outlier of 25 110 m^3/s, which is plotted outside the scale on the y-axis. For comparison reasons a RACMO scenario with the delta change approach (method 1) was constructed as well (Section 3.3.1, Figure 3.2). In Figure 3.10d, RACMO (method 1) and Wp (method 1) are plotted relative to the control climate, where it can be seen that the Wp scenario results in higher extreme discharge levels than RACMO (method 1). When Figure 3.10c and 3.10d are compared, it can be seen that RACMO (method 3) projects the most extreme scenario of increase in flood-peak probabilities. Table 3.7 summarizes information that can be obtained from Figure 3.10 for several return periods at Lobith. Presented flood peaks and their probabilities are calculated based on their GEV fits, which are also shown in Figure 3.10. The RACMO (method 1) and Wp (method 1) scenarios indicate an increase of the 1250-year event from 16 216 m^3/s to 17 492 and 18 729 m^3/s, respectively. The RACMO (method 3) scenario projects a considerably larger increase to 22 372 m^3/s. From Figure 3.10 it is obvious, though, that the RACMO (method 3) GEV fit is highly influenced by the maximum obtained flood peak of 25 110 m^3/s, which seems extraordinarily large. Our hypothesis is that this is an extreme event that is less probable than once in 1000 years.

In Section 3.5.2 we discussed the likely overestimation of events above 12 000 m^3/s at Lobith when using bias-corrected RACMO (method 3) for the control climate period (Figure 3.10b). In an attempt to correct for the overestimation of RACMO (method 3), we present relative values of projected changes in flood peaks in Table 3.8, calculated from the absolute numbers in Table 3.7. First displayed is the relative change in %, where RACMO and Wp (method 1) are compared to 'Control climate CHR (method 1)' and RACMO direct is compared to 'Control climate RACMO'. In this way, we correct for the overestimation of RACMO for the control climate. These relative changes in % are then used to calculate the discharges displayed in the second part of Table 3.8. RACMO (method 1) and Wp (method 1) are thus unchanged, but RACMO direct (method 3) is changed. The RACMO values obtained in this way ('relative' RACMO (method 3)) resemble much more the Wp (method 1) scenario than the RACMO (method 1) scenario. 'Relative' RACMO bias-corrected and Wp delta indicate a peak discharge increase of 12.7–17.3% for all return periods, whereas RACMO delta indicates a shift of 7.9–8.9%.

The extreme value plots in Figure 3.10 and the calculated parameters of the GEV fits can also be used to calculate the projected relative shifts in probabilities of certain events. According to the 'relative' RACMO scenario (method 3) a discharge at a return period of 1250 years in the control climate situation would occur once in 460 years in 2050. This is equivalent to an increased probability with a factor 2.7. The RACMO (method 1) scenario projects that the 1250-year discharge will increase in frequency to once in 510 years (factor 2.5), and the Wp (method 1) scenario projects an increased frequency to once in 265 years (factor 4.7).

Lenderink et al. (2007a) used 90 years of simulated discharge to estimate extreme peak flows at a return period of 100 years for the year 2100, and found an increase between 10 and 30%. If we assume linear interpolation to scale these numbers back to the year 2050, these results are comparable to our results, while Lenderink et al. (2007a) used different climate and hydrological models and different emission scenarios than we did. They compared bias-corrected direct RCM model output to force their hydrological model with the delta change approach, which is partly similar to our methodology. However, they applied the delta change approach to bias-corrected reference data in the control climate, instead of observed values as we did. Shabalova et al. (2003) and Buishand and Lenderink (2004) also obtained comparable results for the year 2100. These studies, like earlier work from Kwadijk and Middelkoop (1994) and Kwadijk and Rotmans (1995), gave basin-wide estimations on projected changes in flood-peak probabilities. Kleinn et al. (2005) used the RCM CHRM, and the hydrological model WaSiM, to derive flood-frequency curves at the sub-basin scale in the Rhine basin, but they did not simulate future climate change projections.

Results at sub-basin scale

In addition to basin-wide projections, we calculated flood peak probabilities for seven sub-basins and analyzed the spatial variation of the results. Table 3.9 shows that the relative change in peak discharge due to climate change increases with increasing return period in all sub-basins, except for the Neckar, where the RACMO (method 3) scenarios depicts a decrease with increasing return period. For the return period of 200 years, resulting values are shown in Figure 3.11. RACMO (method 1) and Wp (method 1) show less spatial variation than RACMO (method 3); this can be expected since the delta change approach (method 1) is uniformly applied to the river basin. The major differences arise in the Main, Mosel and Lahn sub-basins. In the Mosel, RACMO (method 3) projects an increase of almost 40% at a return period of 200 years, while RACMO (method 1) and Wp (method 1) show increases of 10 and 17%, respectively. Comparable differences are found for the other return periods. In the Main and the Lahn the differences between the scenarios vary between 10 and 40%, and 6 and 32%, respectively. In the RACMO (method 3) scenario, for example, the upstream part of the Rhine will not face a large increase in flood-peak probability

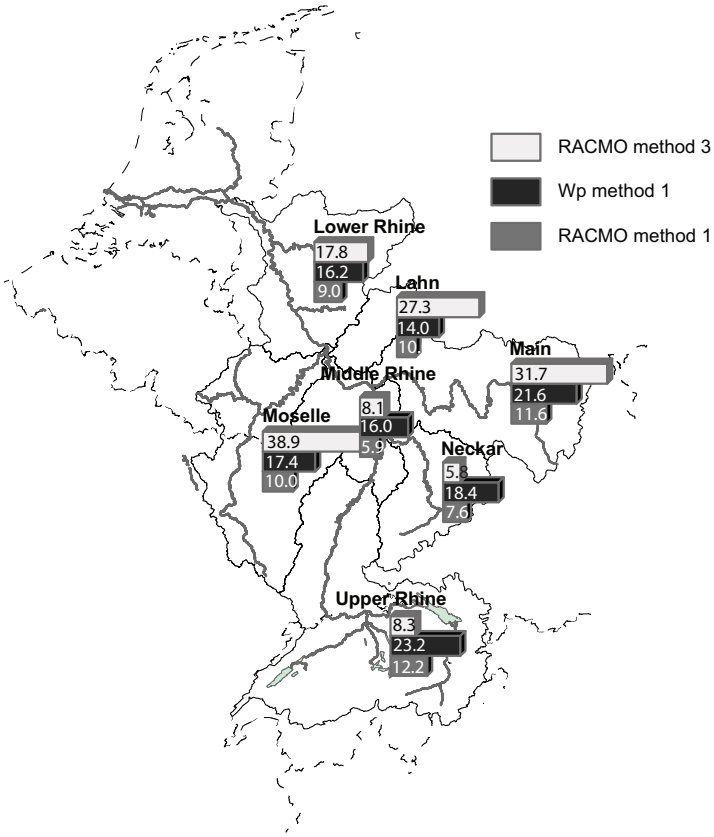

Figure 3.11: Simulated change in discharge (%) at T=200 year at sub-basin scale for the bias-corrected RACMO scenario (method 3) and Wp and RACMO scenarios obtained by the delta change approach (method 1).

Table 3.9: Relative change in discharge at all sub-basins at different return periods (T) under climate change.

Basin	Gauge Discharge	(%)	T (yr) 10	50	100	200	500	1250
Mosel	Cochem	RACMO (mth 1)	7.8	9.0	9.5	10.0	10.7	11.3
		Wp (mtd 1)	15.1	16.3	16.9	17.4	18.1	18.8
		RACMO (mtd 3)	28.7	34.3	36.6	38.9	41.9	44.9
Lahn	Kalkofen	RACMO (mtd 1)	7.1	6.5	6.3	6.2	6.0	5.8
		Wp (mtd 1)	14.3	14.1	14.0	14.0	13.9	13.9
		RACMO (mtd 3)	20.1	23.9	25.6	27.3	29.6	32.0
Main	Raunheim	RACMO (mtd 1)	10.0	10.8	11.2	11.6	12.1	12.7
		Wp (mtd 1)	22.3	22.0	21.8	21.6	21.3	21.0
		RACMO (mtd 3)	20.8	26.1	28.8	31.7	35.9	40.2
Neckar	Rockenau	RACMO (mtd 1)	7.5	7.6	7.6	7.6	7.6	7.6
		Wp (mtd 1)	18.2	18.4	18.4	18.4	18.3	18.1
		RACMO (mtd 3)	10.5	8.1	7.0	5.8	4.1	2.4
Upper Rhine	Maxau	RACMO (mtd 1)	7.0	10.0	11.1	12.2	13.7	15.1
		Wp (mtd 1)	16.0	20.3	21.8	23.2	24.8	26.4
		RACMO (mtd 3)	7.1	8.0	8.2	8.3	8.2	8.2

due to climate change, but in some areas of the Lower Rhine the increase will be higher than the basin-wide projections. The Wp (method 1) scenario, on the other hand, projects the major change in the upstream part of the Rhine basin and projects slightly less changes in the Middle and Lower Rhine.

3.6 Discussion

The aim of this Chapter was to enhance the simulation of future low probability flood-peak events in the Rhine basin. We used an approach that enabled us to use RCM data and a weather generator to create long, resampled time series of climate change scenarios as input for hydrological (daily) and hydro-dynamic (hourly) modeling for the Rhine basin. We applied this approach on three parallel modeling methods, each having a different transformation method of climate data (delta change (method 1), RACMO direct (method 2) and RACMO bias-corrected (method 3)) of different RCM outputs to hydrological model input.

We used resampled meteorological time series up to 1000 years to create long series of daily discharge in order to estimate low probability flood-peak events, without extrapolating extreme value distributions. Extreme value analysis on these data resulted in a GEV distribution to describe the probability distribution instead of the commonly used Gumbel distribution at Lobith (Te Linde and Aerts, 2008). Increased sample

size from 100 years of observed data to 1000 years of simulation results reduced the statistical uncertainty related to distribution fitting, and the extrapolation of those fits, from 13 to 3%. At a return period of 100 years, the estimated peak discharge at Lobith was $13\,000 \pm 1750\,m^3/s$ using only 100 years of observed data, which we reduced to $\pm 440\,m^3/s$ when using a resampled series of 1000 years of climate data. We further recommend using a combination of hydrological modeling and a hydrodynamic model in order to properly simulate flood wave propagation and to address planned measures and structures in the main channel of the Rhine as suggested by Lammersen (2004) and Te Linde and Aerts (2008).

Evaluating simulated precipitation and temperature by direct ECHAM5 forced RACMO2.1 output for the control climate period (1961–1995) revealed a moderate performance by the RACMO RCM. After bias- correction the performance of the RACMO output increased considerably when compared to the observed values, both for seasonal means and extreme values. We saw that an error in the forcing data (direct RACMO output) of +20% (median) propagates to an overestimation of median simulated discharge of 23% compared to observed values, thus stressing the need for bias correction of meteorological data. With bias-corrected RACMO output we succeeded in obtaining realistic mean seasonal discharges in the present climate, both at the basin-wide and sub-basin scales. Other statistical descriptors, such as the standard deviation and skewness, were also well represented at both basin-wide and sub-basin scale.

We identified an underestimation of the most extreme yearly maximum 10-day precipitation events before bias correction for the control climate period (1961–1995), whereas the yearly maximum discharge values were overestimated before bias correction for the same period. This contradicts the common assumption that yearly maximum values of 10-day precipitation and discharge are closely related. We explained this by the observation that the yearly maximum 10-day precipitation events occurred in all seasons, while the yearly maximum discharges mainly occurred in winter, but a thorough interpretation requires further work. The overestimation of yearly maximum discharges before bias correction was in line with the overestimation of daily values of both precipitation and discharge. However, after bias correction the overestimation of peak discharges generated by RACMO (method 3) was reduced. At flood peaks with very low probability (i.e. return periods more than 500 years), discharges obtained by RACMO (method 3) were overestimated by 8–25% for the control climate period. Hay et al. (2002) observed comparable differences in simulated and observed discharge when they used direct RCM output for hydrological simulation in three snowmelt-dominated basins in the United States, and concluded that their RCM, even after bias correction, did not contain the day-to-day variability present in observed precipitation that is necessary for basin-scale hydrological modeling. Lenderink et al. (2003) already recognized an overestimation in daily precipitation values in the winter season by an earlier version of RACMO. Future work

will continue to develop methods to remove biases, where more emphasis is needed on extreme events.

When considering the effect of climate change on mean monthly discharge, the RACMO scenario showed an increase of 14.2% in winter and a decrease of 17.4% in the summer months. This was comparable to the range of the four KNMI'06 scenarios that showed a maximum projected increase in winter by 13.0% and a change in mean summer discharge of +3.0 to −33.3%. Comparing the KNMI Wp scenario and RACMO output at a sub-basin scale, RACMO showed more geographical differentiation in relative contribution between sub-basins than KNMI Wp. This is most likely a direct result from the geographical variation in direct RACMO output, compared to the uniformly distributed delta change approach that was applied to the KNMI Wp scenario.

We have shown that RACMO (method 3) led to surprising results when absolute values of extreme discharges were considered under climate change. The GEV fit was highly influenced by the maximum obtained flood peak of 25 110 m^3/s. Our hypothesis is that this is an extreme event that is less probable than once in 1000 years. Estimates of the Q_{1250} in 2050 in earlier studies on climate change in the Rhine basin never reached more than 20 000 m^3/s at Lobith (Vellinga et al., 2008). We therefore continued to compare relative values of projected changes in flood peaks, to correct for the overestimation of RACMO (method 3). On the basis of 1000-year simulation results, RACMO direct (method 3) and Wp (method 1) indicated a peak discharge increase in 2050 of 12.7–17.3% for return periods between 10 and 1250 years, whereas RACMO delta (method 1) indicated a shift of 7.8–8.9%. Our results projected that a flood-peak event with a return period of 1250 years in the control climate situation will increase its frequency in 2050 according to a variety of scenarios: once in 460 years (factor 2.7, RACMO direct); once in 510 years (factor 2.5, RACMO delta); and once in 265 years (factor 4.7, Wp), in 2050.

At the sub-basin scale, RACMO (method 1) and Wp (method 1) showed less spatial variation than RACMO direct in estimated flood-peak volumes under climate change. Again, this results from the geographical differentiation across the Rhine basin in direct RCM output. The major differences arose in the Main, Mosel, and Lahn sub-basins. In the Mosel, bias-corrected RACMO (method 3) projected an increase of almost 40% at a return period of 200 years, while RACMO direct (method 1) and Wp (method 1) displayed increases of 10 and 17%, respectively. In the RACMO (method 3) scenario, for example, the upstream part of the Rhine will not face a large increase in flood-peak probability due to climate change, but in some areas of the Lower Rhine the increase will be higher than for the basin- wide projections. However, the Wp (method 1) approach projected the largest change in the upstream part of the Rhine basin, and slightly less changes in the Middle and Lower Rhine. These differences

can be of major importance when implementing adaptation measures in relation to climate change, such as detention areas, bypasses, or dike relocations.

A limitation of using RACMO is that the climate change scenario results from one GCM and one RCM, instead of an ensemble of climate models as in the KNMI'06 scenarios. However, as a result of projects such as ESSENCE (Sterl et al., 2007), PRUDENCE (Christensen et al., 2007), and the FP6 ENSEMBLES project (Jacob et al., 2008), more GCM–RCM combinations will become available that can be used to create more resampled and bias-corrected direct RCM climate change scenarios for the Rhine basin. In the current study, this was not feasible. The KNMI'06 scenarios can only be implemented by the delta change approach, but provide a valuable indication of the bandwidth of different climate change projections. This bandwidth can be seen as a delineation of the uncertainty in climate change projections. But KNMI, does not provide an indication on the probability of occurrence of the separate KNMI'06 scenarios (Van den Hurk et al., 2006).

3.7 Conclusions and further work

On the basis of numerous 1000-year model simulations the results indicate a basin-wide increase in peak discharge of the Rhine in 2050 of 8% to 17% for probabilities between 1/10 and 1/1250 years. The results, furthermore, show that increasing the length of the climate data series using a weather generator reduced the statistical uncertainty when estimating low probability flood-peak events from 13% to 3%.

When evaluating future climate, the delta change approach to create climate change scenarios is more transparent than using bias-corrected RCM output. It is a robust method that makes it possible to use output from climate models, even when these climate models do not represent the control climate accurately (Grabs, 1997). However, we are convinced that the use of bias-corrected RCM output is to be preferred in climate change analysis since it incorporates projections of geographical differentiation, and changes in the variance of temperature, the coefficient of variation of precipitation, and the number of precipitation days. Our results are in line with Lenderink et al. (2007a) who also found that direct RCM output was more suitable in a hydrological impact study than the delta change approach using the HadRM3H RCM. But the bias-correction can be improved, especially concerning extreme events. In addition, the use of a rainfall generator in combination with hydrological and hydrodynamic modeling is recommended when simulating low probability peak discharges under climate change. Lengthening the 1000-year model simulations to 2000 years or more, would further improve the simulation of extreme events with a probability of once in 1250 years.

Both scientists and policy makers recognize the inherent uncertainty associated with performing flood risk analysis within climate change scenario studies (Prudhomme et al., 2003; Menzel et al., 2006; Hingray et al., 2007; Pitman and Perkins, 2007), and policy makers struggle on decision-making related to climate change (e.g. Middelkoop et al., 2004). When identifying future problem areas and potential adaptation measures, it is of major importance to be able to estimate spatial differences in flood-peak probabilities. Our results demonstrate that bias-corrected direct RCM output, in combination with the use of a weather generator, can help to meet this requirement.

Further work might focus on analyzing flood peaks in more detail, to gain insight on changes in timing of all sub-basins and how timing influences the ultimate flood peak, with a focus on snowmelt related peak discharges in the Alpine region (see also Stewart (2008)). Work is ongoing to extend the hydrological modeling to 10 000 years, in order to further improve extreme value analysis on peak discharges. Gathering (bias-corrected) GCM and RCM output data of different models to create more climate change scenarios should create insight in the probability of future scenarios, and is already the aim of the international project RheinBlick (information is available at http://www.chr-khr.org/en/projects/rheinblick2050). In addition, low-flow periods deserve more attention in climate change impact studies, since drought risk might be of the same order as flood risk even in temperate climate zones. Finally, in the current situation in the Rhine basin, safety levels vary to such an extent that flooding is likely to occur upstream in Germany, while flood stages do not reach dike heights in the Lower Rhine and in the Netherlands. This effect probably influences discharge peaks and the impact of upstream flooding should be investigated in relation to projected changes in flood-peak probabilities due to climate change scenarios.

Acknowledgements

This research was supported by the project ACER (A7) under the Dutch BSIK Climate Changes Spatial Planning program. We wish to thank Hendrik Buiteveld and Rita Lammersen from the Ministry of Transport, Public Works and Water Management and the German Federal Institute of Hydrology (BfG) for both allowing the use of the HBV and SOBEK models, and providing meteorological (CHR) and discharge measurement data. Marcel Ververs and Simone Patzke from Deltares are kindly acknowledged for their support on the development of the hydrological modeling cascade (GRADE). We also thank Bart van den Hurk (KNMI) and colleagues from the IVM PhD peer group for their constructive comments that helped to improve this Chapter. Finally, we thank Dennis Lettenmaier and two anonymous reviewers for their comments on an earlier version of the Chapter.